CNWRA 94-015

STRATEGY FOR THE EVALUATION AND USE OF PROBABILITY MODELS FOR VOLCANIC DISRUPTIVE SCENARIOS

Prepared for

Nuclear Regulatory Commission
Contract NRC-02-93-005

Prepared by

Center for Nuclear Waste Regulatory Analyses
San Antonio, Texas

June 1994

STRATEGY FOR THE EVALUATION AND USE OF PROBABILITY MODELS FOR VOLCANIC DISRUPTIVE SCENARIOS

Prepared for

Nuclear Regulatory Commission
Contract NRC-02-93-005

Prepared by

Charles B. Connor
Brittain E. Hill

Center for Nuclear Waste Regulatory Analyses
San Antonio, Texas

June 1994

ABSTRACT

Numerous types of probability models have been proposed for volcanic disruption of the candidate high-level nuclear waste (HLW) repository site at Yucca Mountain, Nevada. The precision and accuracy of these models in representing volcanic processes need to be quantified and assessed objectively as part of the license application review and Performance Assessment. The proposed strategy for evaluation and use of probability models requires: (i) quantification of data and model precision, (ii) validation of fundamental model assumptions, (iii) utilization of the same basic geologic data in different conceptual models, (iv) application of models to different periods of time in the Yucca Mountain region (YMR) to evaluate reproducibility of known spatial and temporal patterns of volcanism, and (v) application of models to relatively large volcanic fields that are reasonably analogous to the YMR to evaluate reproducibility of known spatial and temporal patterns of volcanism. The proposed strategy will allow fundamental conceptual differences to be distinguished from variations in the basic data used in the models. Probabilities from evaluated models will be associated with a confidence interval that represents the precision and accuracy of the model. Differences or similarities between model results can then be objectively evaluated for significance. Although current probabilities of volcanic disruption at times appear similar, most of these models have yet to be systematically evaluated. Models that violate known geologic relationships or appeal to unreasonable assumptions may need to be excluded from probability calculations during the license application review.

CONTENTS

FIGURES

TABLES

ACKNOWLEDGMENTS

We thank Dr. Chris Condit for his numerous discussions on the Springerville Volcanic Field and for sharing his compilation of age determinations. The quality of this report was improved from technical reviews by Drs. Randy Manteufel, H. Lawrence McKague and Budhi Sagar, and an editorial review by Mr. Corky Gray. We also thank Ms. Cathy Garcia, Ms. Esther Cantu, and Ms. Peggy Hunka for their valuable technical assistance in the preparation of this report.

This report was prepared to document work performed by the Center for Nuclear Waste Regulatory Analyses (CNWRA) for the Office of Nuclear Materials Safety and Safeguards (NMSS) Nuclear Regulatory Commission (NRC) under Contract No. NRC-02-93-005. The activities reported here were performed on behalf of the NRC Office of Nuclear Materials Safety and Safeguards, Division of Industrial and Medical Nuclear Safety. This report is an independent product of the CNWRA and does not necessarily reflect the views or regulatory position of the NRC.

1 INTRODUCTION

The Yucca Mountain region (YMR) has been the site of recurring small-volume basaltic eruptions during the last 10 my (Crowe et al., 1982; Smith et al., 1990). This volcanic activity has led to the formation of numerous cinder cones, eight of which are less than 1.6 my old. Because of this volcanic activity, it is necessary to evaluate the potential for volcanic disruption of the candidate high-level radioactive waste (HLW) repository at Yucca Mountain. It has been promulgated as part of 10 CFR 60 that this evaluation will include the application of probabilistic methods to estimate the potential for repository disruption during the isolation period (at least 10,000 yr). To date, numerous probability models have been proposed (Crowe et al., 1982, 1993; Smith et al., 1990; Ho, 1991; Ho et al., 1991; Margulies et al., 1992; Sheridan, 1992; Connor and Hill, 1993). Collectively, these models have indicated that the probability of volcanic disruption of the candidate repository is likely greater than 1 in 10,000 in 10,000 yr, indicating that volcanism is of regulatory concern. Substantial differences among these models exist in terms of the basic assumptions made in the calculations, use of available data and estimates of uncertainty in these data, and estimates of the probability of volcanic disruption of the site. The goal of this study is to develop a strategy for probability model evaluation and use that provides a consistent and defendable framework for addressing regulatory issues related to igneous activity.

Direct comparison of probability models developed at the Center for Nuclear Waste Regulatory Analyses (CNWRA) (e.g., Connor and Hill, 1993), the Nuclear Regulatory Commission (NRC) (Margulies et al., 1992), the U.S. Department of Energy (DOE) and its contractors, particularly Los Alamos National Laboratory (LANL) (e.g., Crowe et al., 1982, 1993), and other research groups (Smith et al., 1990; Ho, 1991; Ho et al., 1991; Sheridan, 1992; McBirney, 1992) is an important task in preparation for review of a license application. Because different groups will likely continue to use different models, the NRC will need to evaluate the strengths and weaknesses of individual models and compare model applications with the available data and associated uncertainties. This evaluation must be done in an objective and reproducible fashion, using techniques that are sufficiently robust to handle the complexity of existing and potential new models.

Two related tasks can provide a basis for probability model evaluation: (i) direct comparison of probability models using data from the YMR, primarily with the goal of determining and evaluating differences in calculations of the probability of volcanic disruption among these models in a systematic way, and (ii) comparison of models using data collected from other volcanic fields, primarily with the goal of bounding uncertainties in parameter estimation (precision and accuracy) associated with the application of these models. These two tasks can provide a basis for the development of a strategy for the use, integration, and rejection of various probability models in technical assessment of repository performance and related licensing activities.

Initiation of these tasks is timely in light of recent meetings of the Advisory Committee of Nuclear Waste (ACNW), the Nuclear Waste Technical Review Board (NWTRB), and the National Academy of Sciences, in which the application and differences between probability models have been stressed. DOE research has also shifted toward integration of many probability models (Crowe, 1994), initially through the use of cumulative frequency distributions and eventually through the use of expert judgement (Coppersmith, 1994). Comparison of models and delineation of the underlying assumptions in these models is not always straightforward. Cornell (1994) has pointed out that mathematical and geologic complexity is an inherent component in many probability models, especially those that are nonhomogeneous. This complexity, for example, inclusion of indirect and long-term effects of volcanic activity in probability estimates (Connor,

1994), is often necessary (Cornell, 1994) but does complicate evaluation of these models. Furthermore, an increasing number of YMR probability models have been proposed. Although the differences in probability estimates sometimes are apparently small, differences in their assumptions and limitations often are not. Crowe (1994) has proposed developing probability distribution functions by including all of the models proposed, then selecting a confidence interval for the mean probability of volcanic disruption. This technique is similar to that used in seismology (Cornell, 1994). Given that this type of approach may be utilized by the DOE in its license application, study of the limitations of a range of models and evaluation of their differences is an increasingly needed technical assistance activity.

1.1 REGULATORY FRAMEWORK

Evaluation of volcanism probability models will be used to support specific sections of the License Application Review Plan (LARP). Insight into the frequency, distribution, and volume of basaltic magmatism in the YMR, the repository and regional scales of volcanism effects, and the relationship between volcanism and regional tectonic and structural settings, form an integral part of license review. This includes review of site characterization activities (evidence of igneous activity as a potentially adverse condition, LARP Section 3.2.1.9; and impact of volcanism on groundwater movement, LARP Section 3.2.2.7), and the description of overall system performance (assessment of compliance with the requirement for cumulative releases of radioactive materials, LARP Section 6.1). The Compliance Determination Strategy (CDS) associated with evidence of Quaternary volcanism is of Type 5, indicating that independent research must be conducted to evaluate Key Technical Uncertainties (KTUs) associated with volcanism and that volcanism poses a high risk to the NRC of reaching unwarranted conclusions regarding compliance with 40 CFR Part 191 and 10 CFR Part 60.122(c)(15).

Four KTUs related to igneous activity, identified as part of the CDS concerned with evidence of Quaternary igneous activity, have been identified:

- Low resolution of exploration techniques to detect and evaluate igneous features
- Evaluation of spatial and temporal patterns of igneous activity
- Development and use of conceptual tectonic models as related to igneous activity
- Prediction of future system states (disruptive scenarios)

Evaluation of these KTUs requires detailed safety review supported by analyses (Type 4), and independent tests and other investigations (Type 5). In addition to evaluation of these KTUs, independent research in volcanism is needed to provide a basis to question how DOE research will address the probabilities and potential consequences of igneous activity on repository performance and to evaluate DOE's responses to these questions.

1.2 RELATIONSHIP TO OTHER PROJECTS

Relationships between this Office of Nuclear Materials Safety & Safeguards (NMSS) task and other volcanism activities is summarized as a flow chart in Figure 1-1. Primary data gathering activities in CNWRA volcanism research are carried out under the Field Volcanism and Volcanic Systems of the Basin and Range research projects. The Field Volcanism project is primarily concerned with the

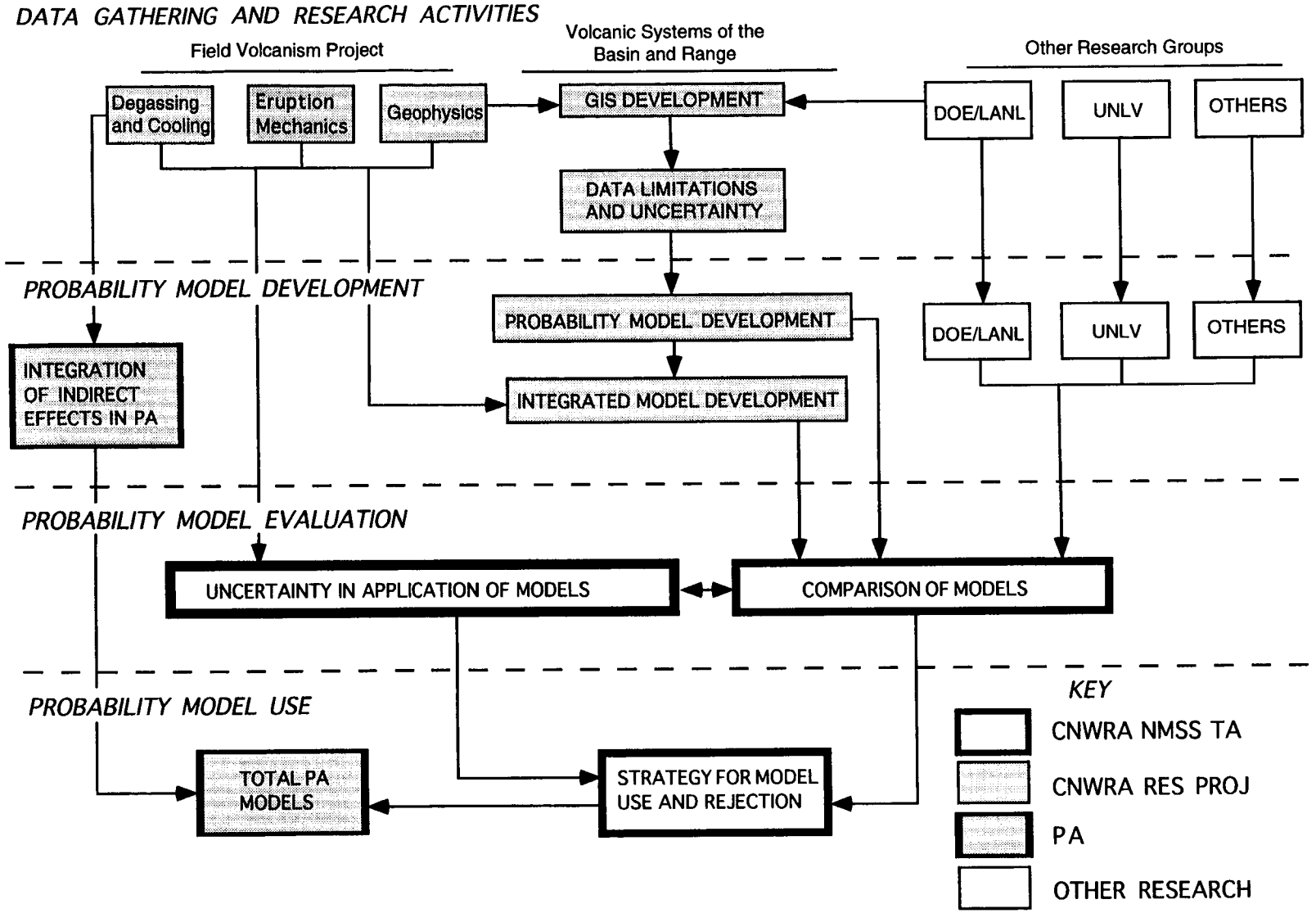

Figure 1-1. Flowchart of activities related to probability model evaluation in use in volcanism

consequences of volcanic activity, including study of the longevity and area affected by cinder cone cooling and degassing; the mechanics of small-volume basaltic volcanism (Connor, 1993); and the area likely disrupted by volcanic activity, primarily investigated through the application of geophysical methods (Connor and Sanders, 1994; McDuffie et al., 1994). The Volcanic Systems of the Basin and Range project encompass investigations in the western Great Basin (WGB) and elsewhere in the Basin and Range with the goal of better understanding patterns of volcanism in this region, and the development of probability models based on these patterns (Connor and Hill, 1993). This research is facilitated through development of a Geographic Information System (GIS) database for the investigation of volcanism (Stirewalt et al., 1992; Connor and Hill, 1994). Assessment of the limitations and uncertainty in relevant geologic data, and the impact of this uncertainty on tectonism and volcanism models for the WGB, is a continuing activity in this project (Hill et al., 1993). Other data that will be included in the GIS are gathered as part of the Field Volcanism project, particularly the Geophysics task, and DOE/LANL research in volcanism. Other groups gathering data for the purpose of probability model development include other DOE contractors, the University of Nevada at Las Vegas (UNLV), and other research groups.

Probability model development is a primary concern of the Volcanic Systems of the Basin and Range research project. Incorporation of other data, such as those gathered in the Field Volcanism project, will likely impact probability models for disruption (Connor and Hill, 1993; McDuffie et al., 1994). This integrated model development, which will include both the results of the probability model development as well as incorporation of insight gained in the Field Volcanism project, will be a primary result of the Volcanic Systems of the Basin and Range project. Other groups, of course, are also involved in probability model development (Crowe et al., 1982, 1993; Smith et al., 1990; Ho, 1992; Sheridan, 1992) (Figure 1-1). A study of indirect effects of volcanic activity on Performance Assessment (PA) models, particularly with respect to hydrologic setting and geochemical transport, is being undertaken as a subtask in the iterative PA activity (Figure 1-1).

The primary focus of this NMSS task is in the evaluation of probability models, where systematic comparison of models and assessment of uncertainty in the application of these models in a regulatory framework will be investigated. Ultimately this will result in the development of a strategy for model rejection or use, which will directly feed into total system PA (Figure 1-1).

Clearly, there is a close relationship between activities in this project and other CNWRA volcanism projects being carried out to assist NRC research. Probability models under development include spatially and temporally nonhomogeneous Poisson models which are discussed in detail in the following sections, spatio-temporal Markov models, and cluster models, including Cox cluster process models. These models, as well as statistical analysis of cinder cone distribution and searches for temporal and spatial patterns in cinder cone volcanism, will be the topic of a FY95 major milestone in the Volcanic Systems of the Basin and Range research project. In addition to these probability and recurrence-rate models, a goal of the Volcanic Systems of the Basin and Range and Field Volcanism research projects is to develop approaches for the incorporation of geologic and geophysical detail into model development. For example, models of the relationship between structural setting and magmatism, both on regional (Parsons and Thompson, 1992) and local (McDuffie et al., 1994) scales, may have an important bearing on the probability of volcanic disruption of the repository. These research projects are oriented toward model development and assessment of regional models, rather than the systematic comparison and evaluation of CNWRA models with those being developed elsewhere.

This division of tasks between NRC Research and NMSS is both appropriate and auspicious. Model development under tasks in the volcanism research projects in no way should be driven or hampered by the need to compare the results with other probability models, current perceptions in the program, or issues of the moment. Such needs would likely stifle the development of models which, for example, may have an important basis in geologic or geophysical concepts, yet do not yield results that are currently deemed significantly different from other models proposed. On the other hand, model evaluation should focus on model comparison, particularly with regard to regulatory limits as they are currently envisaged. This evaluation needs to be broad enough so that results of the analysis may be interpreted without being repeated as changes in regulations are promulgated. Thus, specific comparison of probability models with regard to their performance in accurately forecasting the probability of events such as the formation of new volcanoes, sensitivity studies of the limitations of these models, development of a strategy for model use and integration, and possible rejection of models in licensing activities, are the purview of this NMSS project. In contrast, volcanism probability models are developed and data used in these probability models are assessed under the CNWRA volcanism research programs. For example, spatially and temporally nonhomogeneous Poisson models and their application to the probability of volcanic disruption of the candidate repository have been a topic of research in the Volcanic Systems of the Basin and Range research project. Comparison of this model with, for example, homogeneous Poisson models that have been developed elsewhere (e.g., Crowe et al., 1993), is a proposed part of NMSS technical assistance. Such a division guards against peremptory disregard of a model that may accurately capture the details of a geologic process, but does not yield a probability that is deemed significantly different from a model that is based on other, possibly less robust assumptions.

Naturally, close integration between this NMSS project and PA research is important. Two Iterative Performance Assessment (IPA) subtasks related to volcanism will be implemented in fiscal year 1995. These include a project to modify the volcano code used to model volcanic disruption scenarios in IPA Phase 2 studies (Lin et al., 1993), and model the indirect effects of magma degassing on performance. It is anticipated that the probability model evaluation process will be used in NRC's total performance assessment (Figure 1-1).

2 OUTLINE OF AN EVALUATION STRATEGY

Probability models can be evaluated using procedures that objectively quantify the overall uncertainties associated with each model. Uncertainty in data or models is represented by two distinct components, precision and accuracy. Simply defined, precision refers to how exactly a datum can be measured or constrained. Accuracy, on the other hand, refers to how well the measured value or model represents a given process or parameter. For example, a Quaternary soil may have three dates of 10.9 ± 0.2, 11.1 ± 0.2, and 11.0 ± 0.2 ka. These dates are relatively precise because they have reported errors of about 2 percent and are indistinguishable based on reported analytical error. However, if the age of the dated soil is actually 40 ka, then the high-precision data are essentially useless because they do not accurately indicate the true age of the soil. In contrast, conceptual models relating to basaltic volcanism may be highly accurate but have precisions that are so low as to render them meaningless to HLW licensing issues. For example, a commonly held paradigm is that crustal extension enhances and localizes basaltic magmatism in western North America (e.g., Christiansen and Lipman, 1972; Smith and Luedke, 1984; Armstrong and Ward, 1991). Although this relationship is accurate at regional scales and geologic intervals of time, it is highly imprecise with regards to the candidate repository area and the next 10,000 yr.

Clearly, the precision and accuracy of data and models used in the HLW licensing process need to be assessed independently. For probability models, uncertainty can be quantified objectively through:

- Determination of data precision and accuracy
- Propagation of data uncertainties directly through model calculations
- Evaluation of how accurately probability models reproduce observed patterns of activity through time in the YMR and other well-studied volcanic fields

In addition, it is necessary to evaluate each model using a consistent set of geologic data. Few of the models applied in the YMR have utilized the same basic information regarding volcano location, age, or erupted volume. These models need to be compared using the same data so that the differences in probability estimates are solely a result of differences in model concepts and approaches. This problem is addressed specifically in Section 3.

2.1 PRECISION AND ACCURACY IN PROBABILITY MODEL DATA

Data associated with volcanism studies in the YMR often have large, highly significant uncertainties that must be quantified and minimized if possible. For example, published dates for Red Cone volcano in Crater Flat, Nevada (Figure 2-1), range from 0.95 ± 0.08 Ma (Ho et al., 1991) to 1.9 ± 0.2 Ma (Sinnock and Easterling, 1983). Some of these published dates must be inaccurate, because there is no geologic evidence that Red Cone had eruptions that occurred about 1 my apart (e.g., Smith et al., 1990; Crowe et al., 1993). Dates for Red Cone and other contemporaneous Crater Flat volcanoes average 1.2 ± 0.4 Ma (Hill et al., 1993). The uncertainty associated with this average date significantly affects probability models for future basaltic volcanism in the YMR (Connor and Hill, 1993). However, this uncertainty can be reduced by exclusion of inaccurate or imprecise dates from calculations, and the determination of new dates using higher resolution dating techniques (e.g., Turrin et al., 1991). Inaccurate dates may be identified by confirmatory dating of the previously analyzed samples using higher

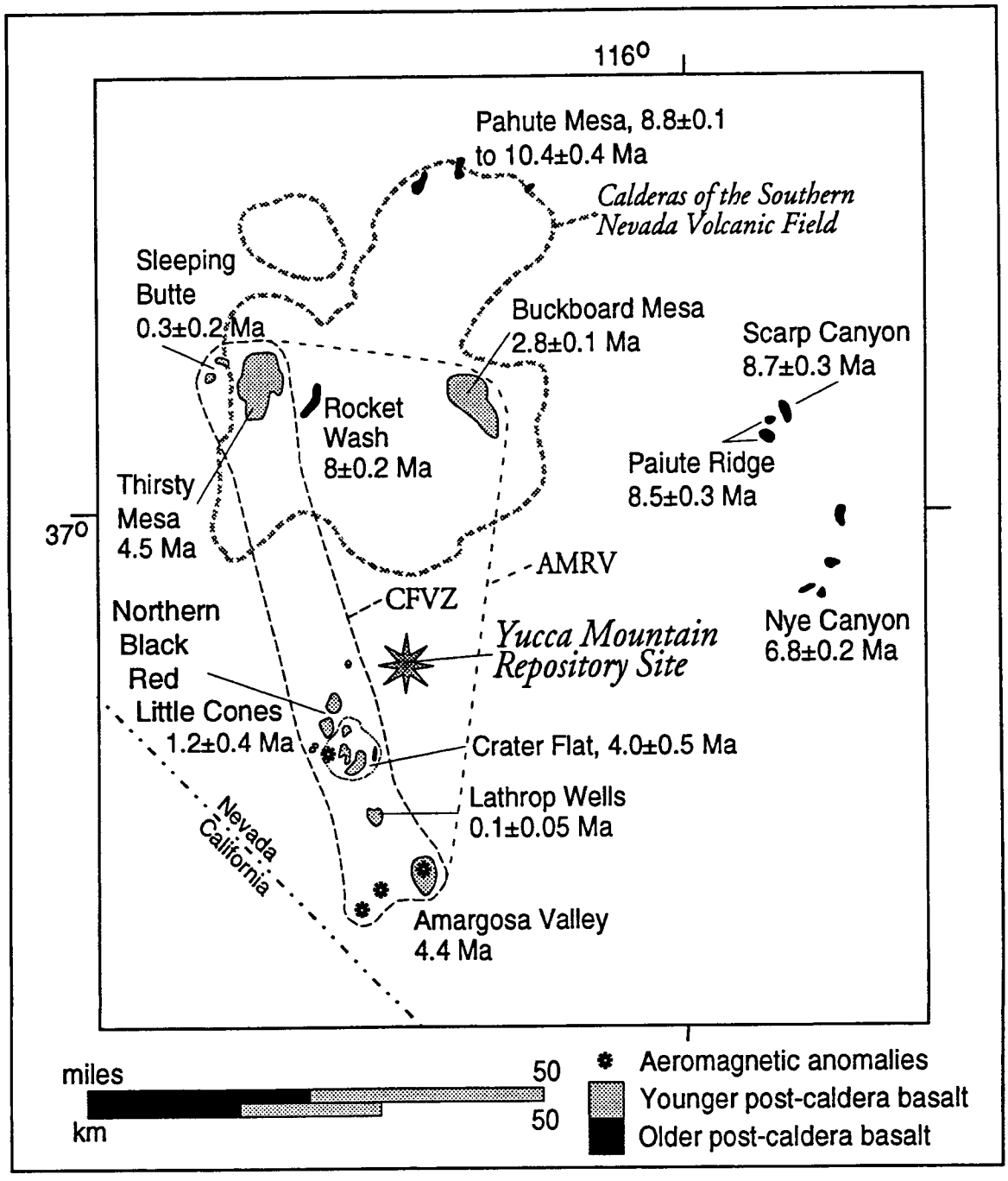

Figure 2-1. Post-caldera basaltic vent locations in the Yucca Mountain Region (modified from Crowe, 1990). Basaltic units are shaded by relative age and mean numeric age is posted (see Table 4-1). Miocene calderas of the Southern Nevada Volcanic Field are outlined by thick dashed lines. The Area of Most Recent Volcanism (AMRV) (Smith et al., 1990) and the Crater Flat Volcanic Zone (CFVZ) (Crowe and Perry, 1989) are outlined. The AMRV has been extended to include the inferred centers of Amargosa Valley. The location of the proposed HLW repository is also indicated (star). Vents inferred from aeromagnetic anomalies are shown by asterisks.

precision dating techniques. Independent assessment of the procedures used to measure the date and suitability of the collected samples for dating also can lead to the rejection of inaccurate or imprecise data. This evaluation is, however, contingent upon having the necessary data presented in papers and reports. Such data are rarely reported (Hill et al., 1993).

Although data uncertainty can be minimized, it cannot be eliminated entirely. This uncertainty must be propagated through subsequent calculations, so that an accurate uncertainty can be assigned to the results of the calculations. Data uncertainty can be propagated using simple arithmetic operations (e.g., Wang et al., 1975). For $A \pm a$ and $B \pm b$, assuming A and B are uncorrelated and a is the standard deviation of A and b is the standard deviation of B:

$$A \pm a + B \pm b = A + B \pm (a^2 + b^2)^{0.5} \tag{2-1}$$

$$A \pm a - B \pm b = A - B \pm (a^2 + b^2)^{0.5} \tag{2-2}$$

$$(A \pm a) \times (B \pm b) = A \times B \pm A \times B \times \left[\left(\frac{a}{A}\right)^2 + \left(\frac{b}{B}\right)^2\right]^{0.5} \tag{2-3}$$

$$\frac{A \pm a}{B \pm b} = \frac{A}{B} \pm \frac{A}{B}\left[\left(\frac{a}{A}\right)^2 + \left(\frac{b}{B}\right)^2\right]^{0.5} \tag{2-4}$$

In addition, if x is well known:

$$(A \pm a)^x = A^x \pm \approx (x \times a \times A^{x-1}) \tag{2-5}$$

Eq. (2-1—2-5) will be used to propagate error through probability calculations. These equations apply as long as the standard deviations are small compared with the measured values, A and B. In the event that this is not the case, higher order terms must be included, and this will increase the calculated variance. As a practical example, the uncertainty associated with an average age of a volcano can generally be represented by the standard deviation of the data set if the uncertainty associated with the dates is small. However, if the uncertainties are large, then these uncertainties must be propagated through the statistical calculations. Using the above relationships and the dates ($X_i \pm x_i$) in Table 2-1:

$$\text{Average} = \bar{X} \pm \bar{x} = \frac{\Sigma X_i}{n} \pm \frac{\left(\Sigma x_i^2\right)^{0.5}}{n} \tag{2-6}$$

In this example, ignoring the uncertainty associated with these dates gives an average date of 0.26 Ma, with a one-standard-deviation uncertainty estimate of only 0.04 Ma (Table 2-1). Note, however, that the error associated with the five individual dates ranges from 38 to 92 percent and averages 57

$$\text{Standard Deviation} = \left[\frac{\Sigma\left(X_i \pm x_i - \overline{X} \pm \overline{x}\right)^2}{n-1}\right]^{0.5} \qquad (2\text{-}7)$$

percent, but the calculated uncertainty on the average date is only 15 percent. This low level of uncertainty does not accurately represent the uncertainty associated with the individual dates, because it only provides the uncertainty in the average. Propagating the uncertainty associated with the individual dates through the calculations results in a standard deviation of 0.05 ± 0.05 Ma. Combining these individual uncertainty terms with the average uncertainty of 0.07 Ma (Table 2-1) yields a combined uncertainty of 0.17 Ma. This uncertainty more accurately represents the 57 percent error associated with the individual dates. Reducing the average date to an appropriate number of significant figures yields an age estimate of 0.3 ± 0.2 Ma, which correctly represents the precision associated with the data.

The Little Black Peak dating example clearly demonstrates why basic data, as opposed to simple averages, need to be reported in order to accurately assess data uncertainties. By ignoring the uncertainty associated with these dates, the simple average and one standard deviation (i.e., 0.26 ± 0.04) yield a false measure of how precisely the age of Little Black Peak is known. Misapplication of this date in probability models would indicate that Little Black Peak was temporally, as well as spatially (Figure 2-1), distinct from the 0.1 ± 0.05 Ma Lathrop Wells eruption (Crowe and Perry, 1991). However, rigorous propagation of the data uncertainty yields an average age of 0.3 ± 0.2 Ma, which indicates that Little Black Peak may be contemporaneous with Lathrop Wells (Hill et al., 1993).

Probability models for YMR volcanism thus can and need to be rigorously assessed by accurately propagating data imprecision through calculations. Calculated probabilities will then have an associated precision that accurately reflects the precision in the model parameters. Current evaluations of the significance of differences in probability model results are qualitative and highly subjective. In contrast, quantified precision can be used to evaluate whether the results from different probability models are statistically distinct for given levels of confidence.

2.2 UNCERTAINTIES IN THE ACCURACY OF PROBABILITY MODELS

In addition to direct comparisons of probability model uncertainties, it is necessary to evaluate the limitations of these models related to the accuracy of assumptions and parameter estimates. This is best determined by applying probability models to other volcanic fields, which formed a greater number of volcanoes and have recognized patterns in volcanic activity.

Central issues related to assessing the accuracy of probability models are:

- Determination that the underlying assumptions of a probability model are reasonable when applied to apparently similar volcanic fields
- Evaluation of model parameters so that the methods used to estimate or constrain the parameters are of sufficient accuracy to represent the studied process
- Quantification of how model parameters need to change in order to apply the model to different volcanic fields

Table 2-1. Compilation of published dates for Little Black Peak, Nevada

Data Source	Date (Ma)	$\pm 1\sigma$ (Ma)	Error (%)
Crowe et al. (1982)	0.29	0.11	38
Crowe et al. (1982)	0.32	0.15	47
Crowe et al. (1982)	0.24	0.22	92
Crowe and Perry (1991)	0.21	0.13	64
Crowe and Perry (1991)	0.22	0.10	45
Average $\pm$ 1σ	0.26 ± 0.05		57
Average with Uncertainty [Eq. (2-6)]	0.26 ± 0.07		
Standard Deviation with Uncertainty [Eq. (2-7)]		0.05 ± 0.05	
Age Estimate considering imprecision	0.26 ± 0.17	(i.e., 0.3 ± 0.2)	

- Comparison between model predictions and observed spatio-temporal patterns of volcanism

Crowe et al. (1982) and others have pointed out that there is a fundamental problem with the application of probability models of volcanic disruption to the YMR. Because there are relatively few volcanoes in the YMR, probability models are often poorly constrained. For many types of probability models, the comparatively few number of volcanoes presents a significant barrier to accurate estimation of model parameters and evaluation of model sensitivities. One approach to addressing these difficulties is to evaluate probability models using data from other, larger volcanic fields. Caution is needed, however, in the use of other volcanic fields because they do not provide a complete volcanological analogy to the YMR. Volcanic fields containing large number of cinder cones, such as the San Francisco Volcanic Field and the Springerville Volcanic Field (SVF), both in Arizona, have tectonic settings that are different from the YMR (e.g., Stirewalt et al., 1992). These tectonic differences likely impact patterns in cinder cone distribution (e.g., Condit et al., 1989). Other volcanic fields in the WGB, such as the Coso Volcanic Field (CoVF) in California, have their own unique characteristics. For example, the CoFV has numerous Quaternary rhyolite eruptions, which are absent from the YMR Quaternary record.

Nonetheless, valuable insights into probability model accuracy can be gained through the analysis of broadly analogous volcanic fields. Three volcanic fields that appear reasonably analogous for applying YMR probability models are the Cima and CoVF in California, and the SVF in Arizona.

2.2.1 Coso Volcanic Field

The CoVF is located in the Coso Range, immediately north of the Garlock fault and east of Owen's Valley in east-central California. Duffield and Roquemore (1988) noted that, unlike other ranges in the region, the Coso Range has a nearly equant shape, indicating that it is the product of perhaps more complex tectonic processes than has led to the formation of the N-S fault blocks of the Inyo Mountains and other ranges in the vicinity.

The CoVF is a bimodal volcanic field, having erupted both primitive basalts and high SiO_2 rhyolites during its history, often penecontemporaneously. Pleistocene eruptions in the CoVF are represented by 38 high-silica rhyolite domes and flows and 14 basaltic centers (Figure 2-2), which range from 1.1 to 0.04 Ma (Duffield et al., 1980). Current activity in the CoVF is limited to geothermal resources found in this area, and fumaroles that occur at the surface along faults cutting younger dacite-to-rhyolite domes. Because of these geothermal resources, the CoVF has been the site of numerous geophysical investigations, largely in an effort to characterize the structure of the field and to image shallow crustal magma bodies in the region using seismic tomographic and related techniques. The CoVF is a good area to test the accuracy of probability models because of the comparatively large number of vents, the spatio-temporal patterns in volcano distribution, and because the relationship to structure is among the clearest of any field in the western U.S.

Duffield et al. (1980) collected and dated 36 basalt and mineral separates in the CoVF. A major conclusion from this study was that volcanism in the CoVF has taken place in essentially two stages. Widespread basaltic volcanism began at approximately 4 Ma with the effusion of basalts over a broad area, which formed an arcuate pattern from southeast to north and west (Figure 2-2). This Pliocene episode lasted until approximately 2.5 Ma. The most recent episode has lasted from 1.1 Ma to approximately 0.04 Ma and was bimodal. Basalts and rhyolites erupted during this period are located in the southern part of the field.

Bacon (1982) found both basalts and rhyolites of the CoVF younger than about 0.4 Ma apparently follow a time-volume predictable pattern. Basalts have erupted at a rate of 2.8 km^3/my since about 0.4 Ma and rhyolites at a rate of 5.4 km^3/my since about 0.25 Ma. Bacon (1982) developed this volume-time relationship using a regression fit on the timing of eruptions and the cumulative volume just prior to eruptions. Extrapolating this regression, a basaltic eruption would be expected in the CoVF sometime in the next 55,000 yr, and a rhyolite eruption would be expected in 60,000 $\pm$ 33,000 yr. Bacon (1982) relates his time-predictable pattern to similar patterns in seismology, suggesting that it results from the increase of some parameter at a constant rate until it reaches a critical point, at which time volcanic eruptions occur. Two parameters that may lead to this type of behavior are pressure in the magma reservoir and extensional strain in the overlying rocks (Bacon, 1982). Bacon (1982) favors a relationship to extensional strain, largely because the CoVF is in an area of active extension. In this model, stress in the crust is accommodated by intruding dikes. The greater the volume of intrusions associated with a given eruptive sequence, the more strain is accommodated. Tectonic strain building at a constant rate will result in a longer period of quiescence between successive eruptions. Bacon (1982) attributes differences in the rates of rhyolitic and basaltic magmatism to differences in the way these magmas migrate through the crust, and therefore differences in the way rhyolite and basaltic intrusions accommodate strain.

Because of bimodal volcanism, the CoVF is not directly analogous to the YMR in several respects. However, the region has been the focus of numerous detailed petrologic, tectonic, and

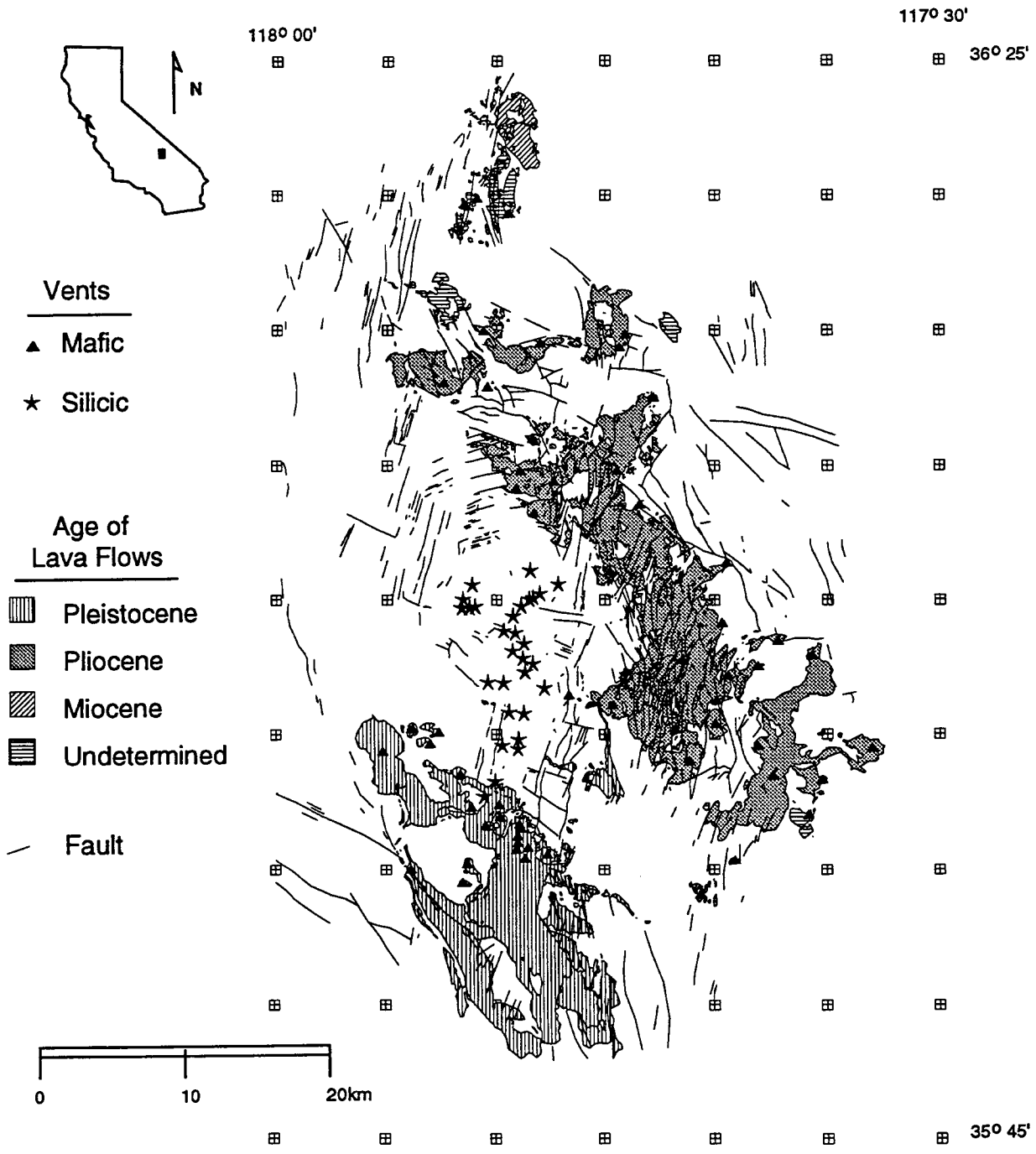

Figure 2-2. Distribution of basaltic and silicic vents, basaltic lava flows, and faults in and around the Coso Volcanic Field. Epoch age is based on K-Ar dates and stratigraphic relationships. Data sources summarized in Connor and Hill (1994).

geophysical investigations. Many of the patterns discerned through these studies may provide a basis for interpretation of similar trends, or simply suggest lines of inquiry for the study of the YMR and more analogous regions located elsewhere in the WGB.

2.2.2 Cima Volcanic Field

The Cima Volcanic Field (CVF) is located in the northeastern Mojave desert, approximately 150 km SSE of Yucca Mountain and 120 km SW of Las Vegas, Nevada. The field is comprised of approximately 40 cinder cones and 60 flows, distributed over an area of approximately 150 km^2 (Figure 2-3) (Dohrenwend et al., 1984, 1986). These features define an episode of volcanic activity that began at approximately 10 Ma and has continued through the latest Pleistocene (Turrin et al., 1985).

The CVF is one of the most studied volcanic fields in the entire WGB. The field was first mapped by Hewitt (1956), who recognized the Quaternary basaltic field and mapped the areal extent of flows. Barca (1965) mapped the southern part of the CVF at a scale of 1:62,000 and Breslin (1982) mapped the youngest cone in the field, Black Tank cone (also known as cone C22) at a scale of 1:2,000. Later studies in the field (Dohrenwend et al., 1984; Wells et al., 1985) augmented these maps and provided details of individual flows and vents. Geochemical and petrologic studies of the field include investigations by Katz (1981), Wilshire (1986), and Farmer et al. (1991). The CVF has been the site of intensive geomorphic studies, calibrated by numerous radiometric age determinations (Dohrenwend et al., 1984, 1986; Turrin et al., 1985; Wells et al., 1985).

Turrin et al. (1985) report 53 high-precision K-Ar dates for the lava flows of the CVF. These data, together with paleomagnetic data collected as part of the same study, provide a very complete record of the timing of basaltic volcanism in this field. Based on these data, Dohrenwend et al. (1984) identified three periods of activity in the field, each lasting approximately 1 my: 7.6 Ma to 6.5 Ma, 4.5 to 3.6 Ma, and 1 Ma to the present. The initial period of activity is only represented by a small volume, highly dissected flow and vent complex located on the southeastern margin of the field (Figure 2-3). Eruptions during 4.5 to 3.6 Ma occurred in the northern half of the field and were the most voluminous. Quaternary eruptions occurred in the southern half of the field (Figure 2-3) and can be further subdivided based on paleomagnetic epochs and the degree of soil development on lava flows from this period (Wells et al., 1985).

The youngest cone in the CVF is the Black Tank cone, located in the extreme SW portion of the field. Katz and Boettcher (1980) and Katz (1981) estimate the age of Black Tank cone to be between 300 and 1,000 yr, based on several lines of evidence. A thermoluminescence (TL) date on the youngest flow from Black Tank was 963 $\pm$ 145 ybp. A date of 860 $\pm$ 130 ybp was reported (Katz and Boettcher, 1980) based on basaltic glass hydration. A ^{14}C date of 330 to 440 ybp was determined for organic matter excavated from beneath the youngest Black Tank flow Katz, (1981). These data, together with the lack of vegetation on Black Tank deposits led Katz (1981) and Breslin (1982) to conclude that Black Tank is quite young. In contrast, Dohrenwend et al. (1986) found evidence to suggest that this cone formed at approximately 15,000 ybp. These data include ^{14}C dates on desert varnish and cation ratio dates (Dorn et al., 1986). All of these dating methods have limitations and are difficult to evaluate without detailed analytical information (Hill et al., 1993). Although this difference in age is interesting from a geochronological point of view, it is trivial for probability model development and testing.

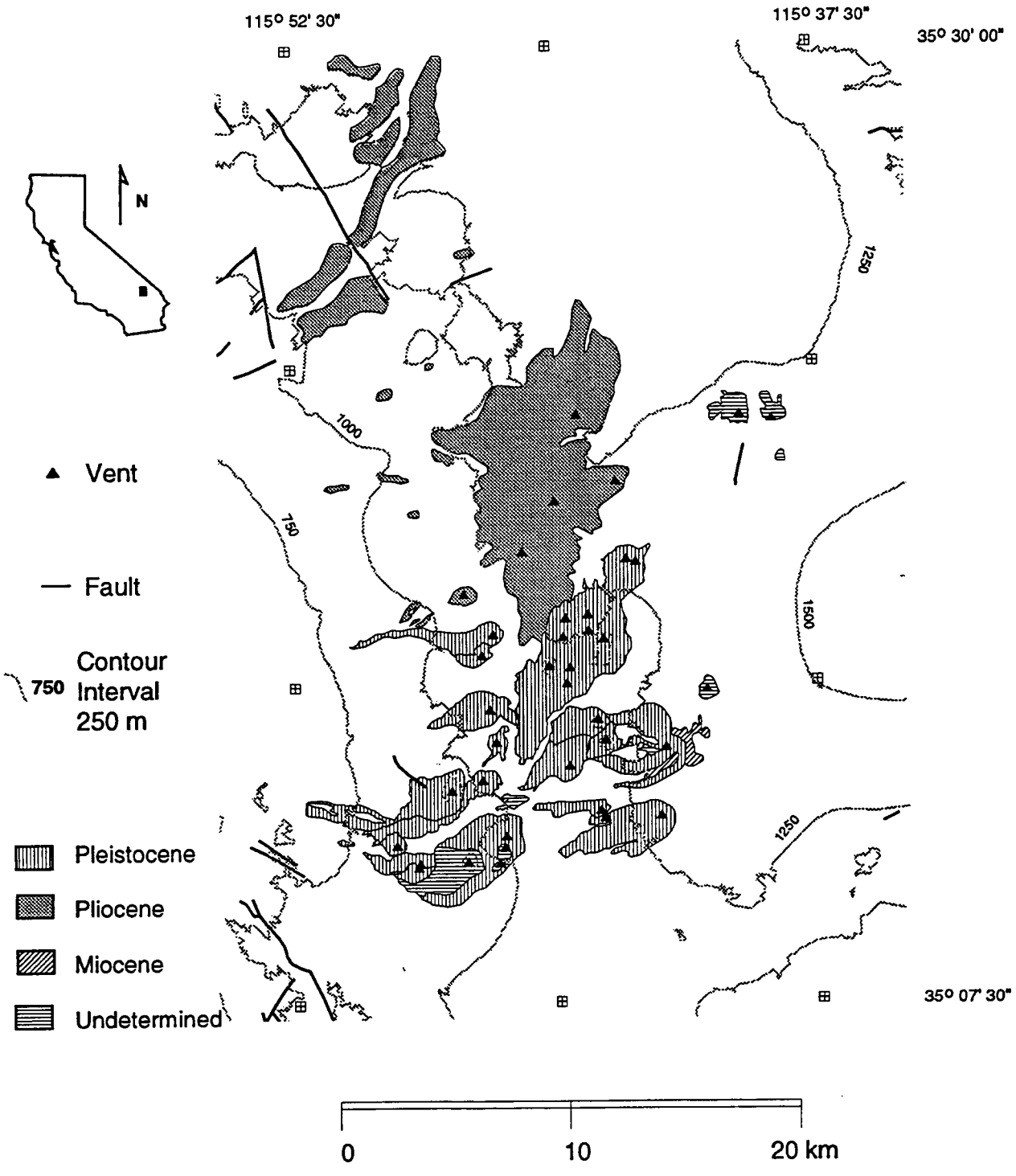

Figure 2-3. Distribution of basaltic and silicic vents, basaltic lava flows, and faults in and around the Cima Volcanic Field. Epoch age is based on K-Ar dates and stratigraphic relationships. Data sources summarized in Connor and Hill (1994).

The abundance of volcanoes and the relatively large number of dates make the CVF an excellent area for the determination of probability model accuracy.

2.2.3 Springerville Volcanic Field

The Springerville Volcanic Field (SVF) comprises approximately 409 vents distributed over an area of about 3,000 km^2 on the southern margin of the Colorado Plateau. Vents in the area consist mostly of cinder cones, but include five maars, four fissure vents, two shield volcanoes, and numerous spatter cones. Geology and geochemistry of the SVF has been discussed by Condit (1984), Condit et al. (1989), and Ulrich et al. (1989). Cooper et al. (1990) have published K-Ar age determinations on SVF lavas. Connor et al. (1992) have discussed patterns in cinder cone distribution in the field, and structural controls on vent alignment evolution. Additional details of the volcanology of this field are given in Section 5 of this report, in which an analysis of the near-neighbor nonhomogeneous Poisson model is made using SVF data.

2.3 USE AND REJECTION OF PROBABILITY MODELS

Many probability models have been proposed for basaltic volcanism in the YMR and will need to be thoroughly assessed as part of the DOE license review. To accomplish this goal, detailed and objective criteria need to be developed to support the use or rejection of probability models in the licensing review and associated PA research. General steps in evaluation processes include:

- Quantification of uncertainties associated with the basic geologic data used to construct the probability models
- Evaluation of model parameters so that the methods used to estimate or constrain the parameters are of sufficient accuracy to represent the studied process
- Propagation of data uncertainties through calculations to associate realistic uncertainties to model results
- Application of different probability models to a consistent data set for the YMR, to evaluate differences in results based exclusively on fundamental differences in the models
- Application of probability models to different periods of YMR basaltic volcanism, to test model accuracy in representing the volcanic history of the region
- Determination that the underlying assumptions of a probability model are reasonable and accurate when applied to volcanic fields that are similar to the YMR
- Quantification of how model parameters might need to change in order to apply the model to different volcanic fields
- Application of YMR probability models to reasonably analogous volcanic fields that have a larger number of volcanoes

It also is apparent that the DOE will develop a set of criteria to evaluate probability models in the license application, and that these criteria also will need to be evaluated in detail. Current indications are that DOE-sponsored research has shifted from emphasizing only a homogeneous Poisson model (e.g., Crowe et al., 1993) toward integration of many probability models (Crowe, 1994). Initially this has been accomplished through the use of cumulative frequency distributions (Crowe, 1994), and will eventually include the use of expert judgement to support or refute specific models (Coppersmith, 1994).

3 CURRENT PROBABILITY MODELS FOR VOLCANIC DISRUPTION

Numerous probability models have been or are currently under development to assess the potential for repository disruption due to basaltic volcanism. These models consist of four primary types:

- Homogeneous Poisson
- Weibull-Poisson
- Near-Neighbor Nonhomogeneous Poisson
- Gaussian

All of these models are Poissonian in their use of Poisson's equation to calculate the probability of volcanic disruption, once recurrence rate has been estimated. The differences among these models arise in estimation of the recurrence rate. These various techniques for estimating recurrence rate can have a substantial impact on estimates of the probability of volcanic disruption of the repository, especially if containment periods longer than 10,000 yr are considered (Figure 3-1). Some details for recurrence-rate estimates are provided in the following sections.

3.1 HOMOGENEOUS POISSON

The simplest approach to recurrence-rate estimation is to average the number of events that have occurred during some time period of arbitrary length and within some arbitrary region. This estimation technique works well for distributions that are completely spatially and temporally random (Cressie, 1991). For instance, Ho et al. (1991) average the number of volcanoes that have formed during the Quaternary (e.g., 1.6 my) to calculate the recurrence rate. Through this approach they estimate an expected recurrence rate of 5 volcanoes/million years (v/my). Crowe et al. (1982) averaged the number of new volcanoes over a 1.8 my period. Crowe et al. (1992) consider the two Little Cones to represent a single magmatic event, and therefore conclude that there are seven Quaternary centers in the region. This lowers the estimated recurrence rate to approximately 4 v/my. The probability of a new volcano forming anywhere in the YMR during the next 10,000 yr is between 4 percent and 5 percent, assuming a regional recurrence rate of between 4 and 5 v/my. As should be evident, the probability determined using a recurrence-rate estimate made in this manner is highly dependent on the area and time scales over which the recurrence rate is estimated. Wallman (1994) summarizes the differences that can arise in probability estimates when recurrence rates are estimated using various area terms. Crowe et al. (1993) have summarized the results of numerous calculations made using estimates of recurrence rate over various areas and time intervals. Some of the areas used by Crowe et al. (1993) and Crowe (1994) are defined using various structural control scenarios and cluster models. McBirney (1992) has illustrated some of the difficulties inherent in the application of homogeneous Poisson estimation techniques to problems in volcanology, such as defining time and area intervals in geologically meaningful ways.

Uncertainties associated with the application of the homogeneous Poisson model, therefore, lie entirely in the selection of area and time-interval terms over which the process is assumed to be random. In cases where there are excellent reasons for choosing a particular area and time interval, for example if it could be shown with some certainty that volcanism can occur only overlying pre-existing structures along which distribution is random, then average recurrence rates may be applied with some confidence. However, these types of criteria have not been developed yet for basaltic volcanoes or volcanic fields.

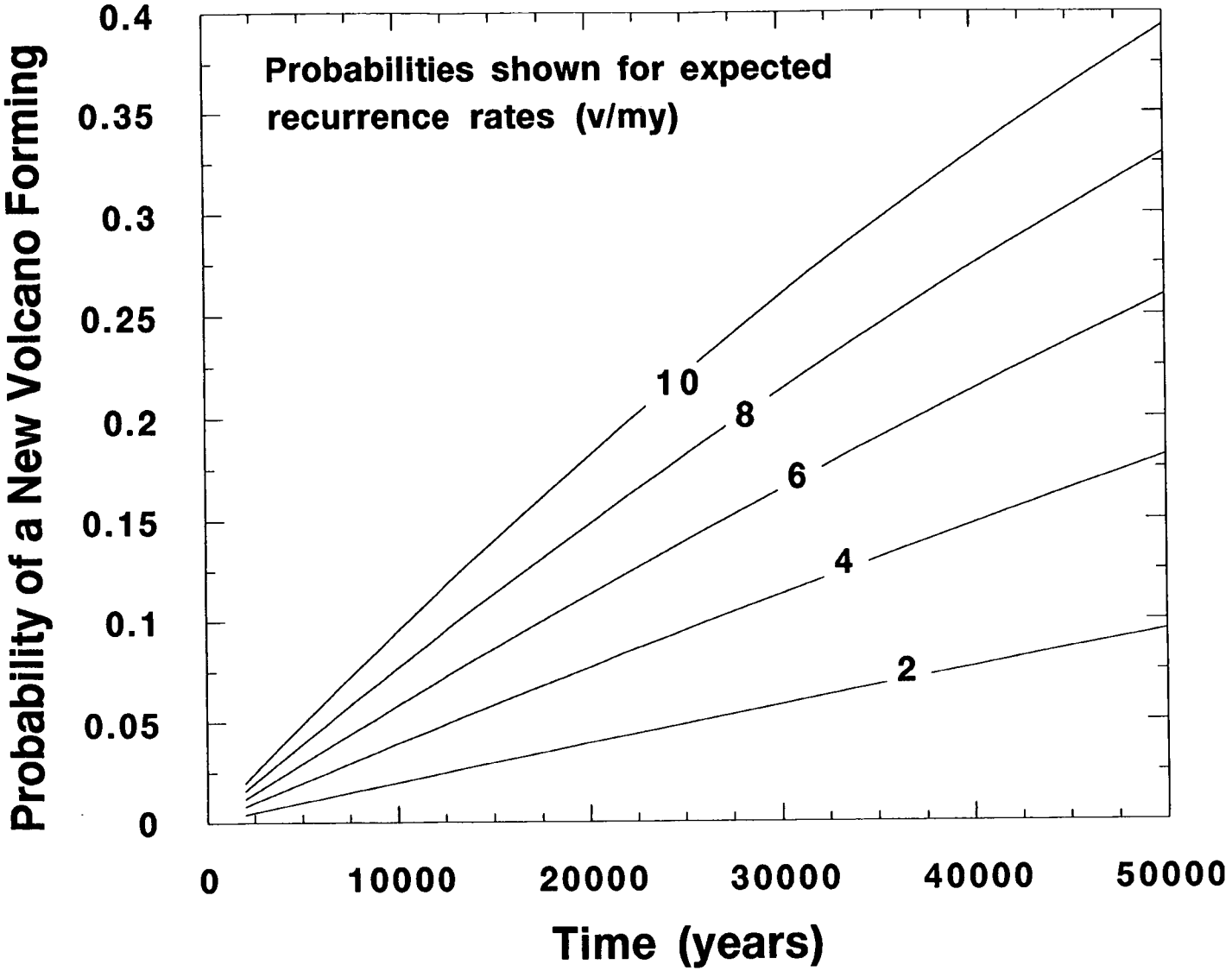

Figure 3-1. Probability of a new volcano forming in a region strongly depends on estimates of the regional recurrence rate (Hill et al., 1993)

3.2 WEIBULL-POISSON

Ho (1991) applied a Weibull-Poisson technique (Crow, 1982) to estimate the recurrence rate of new volcano formation in the YMR as a function of time. Ho (1991) estimates $\lambda(t)$ as:

$$\lambda(t) = \left(\frac{\beta}{\theta}\right)\left(\frac{t}{\theta}\right)^{\beta-1} \tag{3-1}$$

where t is the total time interval under consideration (such as the Quaternary), and β and θ are intensity parameters in the Weibull distribution that depend on the frequency of new volcano formation within the time period, t, and the change in frequency during t. In a time-truncated series, β and θ are estimated from the distribution of past events. In this case there are n=8 new volcanoes formed in the YMR during the Quaternary. β and θ are given by (Ho, 1991):

$$\beta = \frac{n}{\sum_{i=1}^{n} \ln\left(\frac{t}{t_i}\right)} \tag{3-2}$$

and

$$\theta = \frac{t}{n^{1/\beta}} \tag{3-3}$$

where t_i refers to the time of formation of the i^{th} volcano. If β is approximately equal to unity, there is little or no change in the recurrence rate as a function of time, and a homogeneous Poisson model would provide an estimate of regional recurrence rate quite similar to the nonhomogeneous Weibull-Poisson model. If $\beta>1$, a time trend exists in the recurrence rate, and events tend to occur more frequently with time. If $\beta<1$, new volcanoes form less frequently over time and the magmatic system may be waning.

Where few data are available, such as in analysis of volcanism in the YMR, the value of β can be strongly dependent on the period t and the timing of individual eruptions. Ho (1991) analyzed volcanism from 6 Ma, 3.7 Ma, and 1.6 Ma to the present and concluded that volcanism is developing in the YMR on time scales of t=6 and 3.7 Ma, and has been relatively steady, and β=1.1 during the Quaternary.

Uncertainty in the ages of Quaternary volcanoes has a strong impact on recurrence-rate estimates calculated using a Weibull-Poisson model. For example, if mean ages of Quaternary volcanoes are used (Connor and Hill, 1993) and t=1.6 Ma then, as Ho (1991) calculated, β=1.1, and the probability of a new volcano forming in the region within the next 10,000 yr is approximately 5 percent. This agrees well with recurrence-rate calculations based on simply averaging the number of new volcanoes that have formed since 1.6 Ma. However, if older volcano ages are used, for example, if Crater Flat volcanoes are

Table 3-1. Dependence of the Weibull-Poisson model of recurrence rate of volcano formation on age.

Volcano Ages	t (my)	β	θ	λ(v/my) 90% Confidence Interval	P (10,000 yr)
Mean ages[1]	1.6	1.1	0.2	5.4 (1.8, 12.4)	5%
Oldest ages[2]	1.6	0.3	0.001	1.5 (0.5, 3.44)	1.5%
Youngest ages[3]	1.6	2.2	0.6	11.0 (3.7, 25.3)	10%
Mean ages[1]	1.2	0.3	0.002	2.1 (0.7, 4.8)	2%
Varying ages[4]	1.2	0.7	0.2	4.8 (1.6, 11.0)	5%

[1] Volcanoes have mean ages in Table 4-1 (i.e., Black Cone is 1.2 Ma)

[2] Volcano ages are at oldest limits of uncertainty in Table 4-1 (i.e., Black Cone is 1.6 Ma)

[3] Volcano ages at youngest limits of uncertainty in Table 4-1 (i.e., Black Cone is 0.8 Ma)

[4] Crater Flat volcanoes are assumed to vary in age between 0.8 and 1.2 Ma

considered to have formed at 1.6 Ma, then $\beta=0.3$, the magmatic system appears to be waning, and the probability of a new volcano forming during a 10,000-yr confinement period is approximately 1.5 percent (Table 3-1). Conversely, using young volcano ages, $\beta=2.2$, the magmatic system appears to be waxing, and the probability of a new volcano forming within 10,000 yr is approximately 10 percent. Therefore, given the uncertainty in the ages of Quaternary volcanoes in the YMR, it currently is not possible to differentiate between waxing and waning models for the frequency of new volcano formation using the Weibull-Poisson method with a constant time period, t=1.6 Ma.

Crowe et al. (1993) have pointed out that the Weibull-Poisson model is strongly dependent on the value of t, and suggested that t should be limited to the time since the initiation of a particular episode of volcanic activity. This has an important effect on Weibull-Poisson probability models. If mean ages of Quaternary volcanoes are used and t=1.2 Ma, the probability of a new volcano forming in the next 10,000 yr drops from 5 to 2 percent, and $\beta<1$, indicating waning activity (Table 3-1). Alternatively, volcanism along the Crater Flat volcano alignment may have occurred over a period of several hundred thousand years. If volcanism was initiated along the alignment approximately 1.2 Ma but continued through 0.8 Ma, the expected recurrence rate is again close to 5 v/my and the probability of new volcanism in the YMR within the next 10,000 yr is about 5 percent (t=1.2 Ma, Table 3-1). The

confidence intervals calculated on $\lambda(t)$ are quite large in all of these examples due to the few events (n=8) on which the calculations are based. Using the youngest volcano ages for example, the recurrence rate is less than 25 v/my with 90-percent confidence. Using mean ages, the recurrence rate is less than 12 v/my with 90-percent confidence (Table 3-1).

Clearly, determination of the time interval, t is one of the main uncertainties associated with the application of the Weibull-Poisson model. In the past, the Weibull-Poisson method has been applied using homogeneous area terms. That is, once a nonhomogeneous recurrence rate is estimated using the Weibull-Poisson method, it is applied over an area of arbitrary shape and dimensions (Ho et al., 1991).

3.3 NEAR-NEIGHBOR NONHOMOGENEOUS POISSON

Expected recurrence rate per unit area at an arbitrary point within the YMR can also be estimated using varying numbers of near neighbors (Connor and Hill, 1993):

$$\lambda_r = \frac{m}{\sum_{i=1}^{m} u_i t_i} \tag{3-4}$$

where m near-neighbor volcanoes are determined as the minimum, $u_i t_i$, t_i is the time elapsed since the formation of the i^{th} nearest-neighbor volcano, and u_i is the area of a circle with a radius equal to the distance from the i^{th} randomly chosen point to the nearest volcano, where $u_i \geq 1$ km^2. Uncertainty in the use of this model arises in the selection of the number of near neighbors that should be used to estimate the recurrence rate at a particular point and time. Connor and Hill (1993) have demonstrated that estimates of the probability of volcanic disruption of the candidate repository site are strongly dependent on m. One approach is to differentiate between various near-neighbor nonhomogeneous Poisson models by comparing the observed recurrence rate for the region with the expected regional recurrence rate calculated using near-neighbor methods, defined by

$$\lambda_t = \int_X \int_Y \lambda_r(x,y)\,dy\,dx \tag{3-5}$$

where λ_t is the estimated YMR recurrence rate, based on the nonhomogeneous model. In practice, recurrence rates, λ_r, are calculated on a grid and these values are summed over the region of interest

$$\lambda_t = \sum_{i=0}^{m} \sum_{j=0}^{n} \lambda_r(i,j)\Delta x \Delta y \tag{3-6}$$

where Δx and Δy are the grid spacing used in the calculations, and m and n are the number of grid points used in the X and Y directions, respectively. In the YMR, near-neighbor nonhomogeneous Poisson models using six to seven near-neighbor volcanoes give regional recurrence rates of 7 ± 3 v/my (Connor and Hill, 1993). This estimation technique, however, still depends on estimates of the regional recurrence rate, λ_t. Although this dependence can be bounded by choosing a range of recurrence rates (Connor and

Hill, 1993), it nonetheless introduces a degree of uncertainty. Thus, the major sources of uncertainty in application of the near-neighbor nonhomogeneous Poisson model lie in the selection of the number of near neighbors, and, implicitly, the selection of a regional recurrence rate.

3.4 GAUSSIAN MODEL

Sheridan (1992) suggested that the frequency of dike injection may be described by a bivariate Gaussian surface centered on the Crater Flat area or a similar location. The central premise behind this model is that spatial variation in vent and dike distribution is self evident in volcanic fields. Sheridan (1992) chose to account for this variation by assuming that a reasonable mathematical model for a recurrence-rate surface of dike occurrence could be used to estimate probabilities of volcanic disruption of the repository. In the case of a bivariate Gaussian model, the standard deviation and eccentricity of the surface must be estimated. Estimation of these parameters introduces uncertainty in the application of this type of model, as discussed by Sheridan (1992).

3.5 OTHER MODELS

Additional probability models are under development at the CNWRA including Cox cluster models and Markov models. Other groups will likely develop other models as research continues. As mentioned earlier, the incorporation of additional geologic and geophysical data into any of these models will likely become an important part of probability model development at the CNWRA. These models will also have uncertainties associated with them. For example, parameters estimated in the Markov model include estimates of the rate of change in the mean and standard deviation of the locus of volcanism. In preliminary models, these parameters have been estimated by a least-squares fit to the distribution of existing volcanoes, once again resulting in uncertainty in the application of the model.

4 AN EXAMPLE OF PROBABILITY MODEL COMPARISON

Probability models for volcanic eruptions in the YMR need to be compared in a systematic manner. Few of the available YMR probability models utilize the same geologic data, such as volcano location or mean age. In addition, uncertainty in model parameters has not been propagated through any of the current probability models. Thus, differences in model results cannot be attributed to different conceptual approaches to modeling or simply to variations in the data used to apply the model to the YMR. In order to evaluate the significance of differences in probability models, two important tests need to be applied. First, the same basic geologic data needs to be used in the individual probability models. This removes the current variability in model results due to individual variations in the location, age, or volume of igneous features. Second, the same levels of data uncertainty need to be applied to the different models in order to evaluate the sensitivity of the models to different parameter uncertainties (e.g., repository size, area of disruption).

Probability model comparison can be done in several ways. As an example, the homogeneous and nonhomogeneous Poisson models are compared in terms of the differences in recurrence rate. This is accomplished in two steps. First, the mathematical relationship between the two methods of estimating recurrence rate is developed. This is done by comparing estimates of recurrence rate assuming complete spatial and temporal randomness in the sampled population. Second, the two methods are compared using basaltic volcanoes in the YMR. The performance of each model is determined using these existing centers. This provides an overview of the limitations of both methods and the differences in their application. Data used in this comparison are provided in Figure 2-1 and Table 4-1.

The relationship between recurrence-rate estimates in nonhomogeneous and homogeneous Poisson models, in which the recurrence rate is constant over time and within a specified area, can be illustrated by describing the behavior of $\lambda_r(x,y)$ when a completely spatially and temporally random process is sampled. Modifying Eq. (3-4) slightly:

$$z_i = u_i t_i \tag{4-1}$$

$$\lambda_r(x,y) = \frac{m}{\sum_{i=1}^{m} z_i} = \frac{1}{E(Z)} \tag{4-2}$$

where $E(Z)$ is the expected value of z. If volcanoes form as the result of a completely spatially and temporally random process, $E(Z)$ can be thought of as the expected time and area within which n volcanoes will form, and z must have a gamma density distribution (Ripley, 1981). Therefore the probability density function for z is:

$$f_z(z) = \frac{\lambda^n}{(n-1)!} z^{n-1} e^{-\lambda z} \tag{4-3}$$

where λ is the average recurrence rate within some specified area and over some specified time interval. The expected value of z, given this probability density function, becomes:

Table 4-1. Locations of volcanic centers and ages used for statistical models. Vent coordinates in Universal Transverse Mercator, zone 11, Clarke 1866 spheroid. Data sources in Connor and Hill (1993). Reported age uncertainties are calculated using Eq. (2-6 and 2-7).

Name	Age (Ma)	UTM easting	UTM northing	Name	Age (Ma)	UTM easting	UTM northing
Amargosa Valley SW	≈4.4	543376	4048820	Hidden Cone	0.3±0.2	523301	4113698
Amargosa Valley	≈4.4	544817	4050859	Thirsty Mesa	≈4.5	528129	4112249
Amargosa Valley NE	4.4	550306	4053139	Rocket Wash	8.0±0.2	535539	4109028
Lathrop Wells	0.10±0.05	543737	4060073	Buckboard Mesa	2.8±0.1	554946	4109111
Crater Flat S	4.0±0.5	541493	4066057	Pahute Mesa W	10.4±0.4	548758	4133489
Crater Flat E	4.0±0.5	543704	4067644	Pahute Mesa	9.1±0.7	554170	4134467
Crater Flat W	4.0±0.5	540584	4067787	Pahute Mesa E	8.8±0.1	561927	4132182
Crater Flat NW	4.0±0.5	539915	4070959	Paiute Ridge S	8.5±0.3	593698	4101888
Crater Flat W	4.0±0.5	536879	4068573	Paiute Ridge N	8.5±0.3	593611	4103166
Little Cone SW	1.2±0.4	534626	4069423	Scarp Canyon	8.7±0.3	595625	4103906
Little Cone NE	1.2±0.4	534825	4069884	Nye Canyon N	6.8±0.3	603210	4091744
Red Cone	1.2±0.4	537259	4071648	Nye Canyon	6.8±0.3	602370	4085671
Black Cone	1.2±0.4	538257	4074275	Nye Canyon SE	6.8±0.3	600999	4082470
Northern Cone	1.2±0.4	540088	4079455	Nye Canyon SW	6.8±0.2	599557	4083139
Little Black Peak	0.3±0.2	521298	4111346				

$$E(Z) = \frac{\lambda^n}{(n-1)!}\int_0^\infty z^n e^{-\lambda z} dz \tag{4-4}$$

$$E(Z) = \frac{\lambda^n}{(n-1)!}\frac{n!}{\lambda^{n+1}} = \frac{n}{\lambda} \tag{4-5}$$

In order to compare $E(Z)$ with the recurrence rate per unit area, as defined in Eq. (4-2), $E(Z)$ is evaluated for $n=1$, that is, the expected time and area within which one new volcano will form. Combining Eqs. (4-2) and (4-5):

$$\lambda_r(x,y) = \lambda \tag{4-6}$$

for completely spatially and temporally random distributions. The near-neighbor estimate of recurrence rate, $\lambda_r(x,y)$, becomes a constant equal to the average recurrence rate over some specified area if the underlying distribution is completely spatially and temporally random. The near-neighbor nonhomogeneous Poisson model is simply a general form of homogeneous Poisson models. One distinct advantage of using the more general near-neighbor nonhomogeneous Poisson models rather than homogeneous Poisson models is that regions within which λ is taken to be constant need not be arbitrarily defined.

The utility and limitations of the model can be evaluated by determining the effectiveness of the model in forecasting the position and timing of past volcanism in the region. Figures 4-1a to 4-1d illustrate the formation of new cinder cones through time and their corresponding probability maps calculated using the near-neighbor nonhomogeneous Poisson method. For example, Figure 4-1b shows the probability distribution for future volcanism in the YMR calculated at the beginning of the Quaternary and using only pre-Quaternary volcanoes. These maps were calculated using $m=6$ near neighbors, $a=8$ km^2, $t=10{,}000$ yr. The area term, a, is defined to include the repository and a small zone, extending 250 m out from the repository perimeter. Times vary from 5 to 0.1 Ma and were chosen to correspond to periods just prior to the onset of renewed episodes of volcanic activity, providing a conservative test of the probability model. Five million years ago (Figure 4-1a), basaltic volcanism was concentrated east and north of the proposed repository area. Pliocene vents in Crater Flat Valley had not yet formed; these would begin to form about 1 my later. The probability model does not predict the shift of volcanism into the Crater Flat region (Figure 4-1a); and the regional recurrence rate at 5 Ma was approximately 0.7 v/my, about one order of magnitude lower than during the Quaternary. The formation of vents in the Crater Flat area around 4 Ma results in a dramatic change in the probability map, shifting the high-probability contours into the Crater Flat area for the first time. Because no recognized volcanism occurred in the region between the formation of these volcanoes and the later formation of the five 1.2 ± 0.4 Ma cinder cones in Crater Flat, with the exception of the formation of Buckboard Mesa at 2.8 Ma, the regional recurrence rate at the beginning of the Quaternary is about 2.4 v/my; and Crater Flat continues to be the area most likely to experience renewed volcanic activity (Figure 4-1b). Just prior to the formation of the 1.2 ± 0.4 Ma Crater Flat volcanoes, the model indicates that the probability of formation of volcanoes at their locations ranges from $P[N \geq 1, 10{,}000\text{ yr}] = 6\times10^{-5}$ to 1.3×10^{-4}. These are among the highest probabilities in the region at that time. As a result of the formation of the five Crater Flat

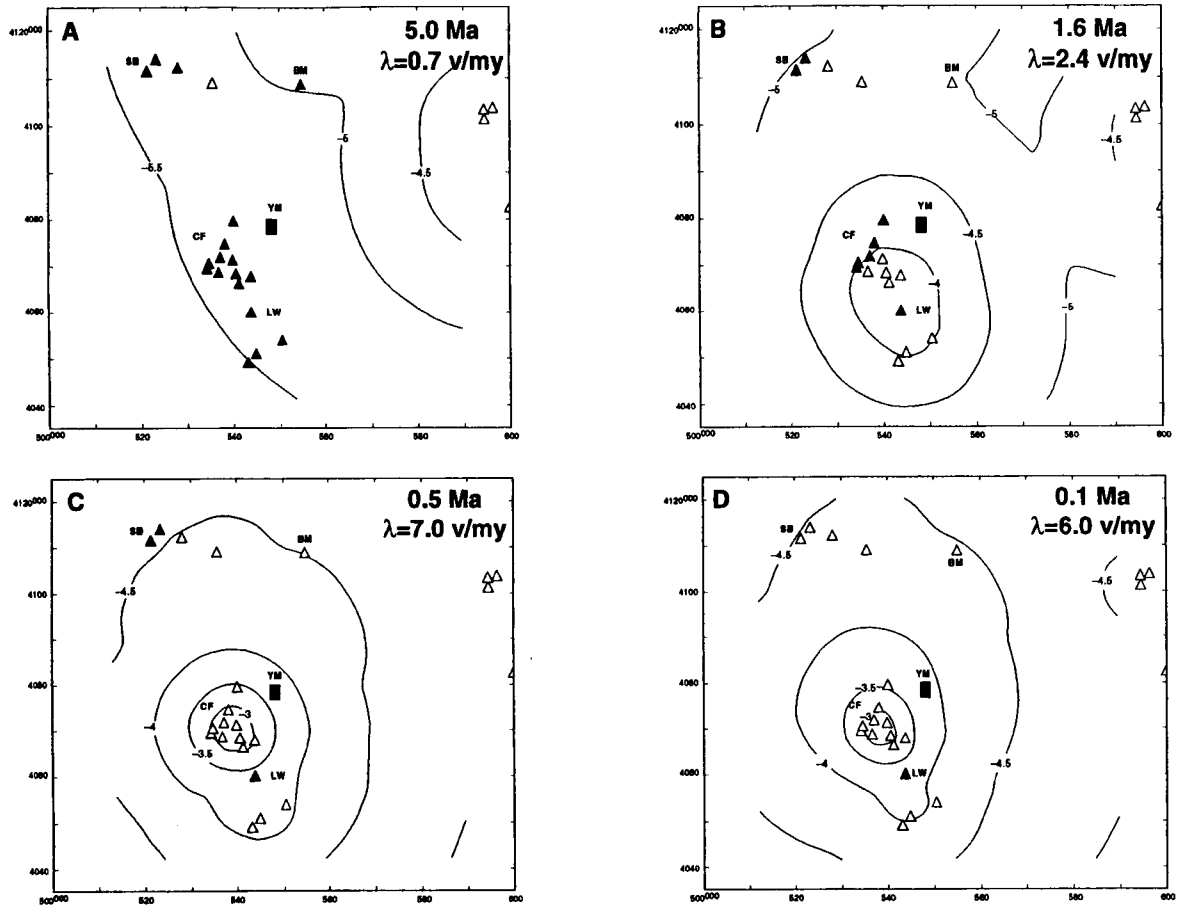

Figure 4-1. Distribution of volcanoes and their corresponding probability maps, as they appeared just prior to the occurrence of additional volcanic activity at (A) 5 Ma, (B) 1.6 Ma, (C) 0.5 Ma, and (D) 0.1 Ma. Probability calculations are based on the distribution and ages of volcanoes formed prior to the time of the calculations (open triangles). Solid triangles show volcanoes that had not yet formed. The contour interval is 0.25 log(P[N≥1, 10,000 yr]) i.e., −4 is a probability of 1×10^{-4} of a new volcano forming within an 8 km^2 area in 10,000 yr. The regional recurrence rate, λ, is shown for each map.

volcanoes, the regional recurrence rate and the probability of renewed activity increase throughout the entire region. However, after the formation of these volcanoes at 1.2 ± 0.4 Ma, there is little change in the shape of the probability distribution through time because of the concentration of relatively young volcanoes within and near Crater Flat. At 0.5 Ma, just prior to the formation of the Sleeping Butte cinder cones (0.3 ± 0.2 Ma), the zone of highest probability is centered on Crater Flat and slightly elongate in a NNW direction due to prior activity north and south of Crater Flat. The probability of volcanism at Sleeping Butte just prior to their formation is low, $P[N \geq 1, 10{,}000 \text{ yr}] = 3.0 \times 10^{-5}$, compared to other areas in the YMR at the time of their formation. Although older volcanoes, such as Thirsty Mesa, are found in the area around Sleeping Butte, fewer than six volcanoes are located in this area; and therefore probabilities are generally low when calculated using $m = 6$ near-neighbor volcanoes. Finally, Lathrop Wells, the youngest cinder cone in the region, forms in an area of comparatively high probability, $P[N \geq 1, 10{,}000 \text{ yr}] = 3.2 \times 10^{-4}$.

Direct comparison of the results of this analysis with the results of homogeneous Poisson models is problematic because homogeneous Poisson models are highly dependent on an area term, A_r, within which the probability is equal everywhere. The selection of A_r is even more precarious where data are clustered (Ripley, 1981; Cressie, 1991). Nonhomogeneous Poisson models do not have this area dependence. For comparative purposes, the results of performance analysis of the nonhomogeneous model in estimating volcano locations in the YMR through time can be compared to homogeneous Poisson models using several different values for A_r. Recall that the performance of the nonhomogeneous model can be evaluated by calculating the probability of a volcano forming at its future position, prior to the formation of this volcano (i.e., Figures 4-1a — 4-1d). The results of this comparison are provided in Table 4-2, together with the regional recurrence rate, λ_r, calculated using $m = 6$ near-neighbor volcanoes. Using these values for λ_r, the probability of a new volcano forming within any 8-km^2 area can be calculated using the homogeneous Poisson model. For the purposes of these calculations, the probability of volcanism outside of A_r is assumed to be zero, maximizing the probability of volcanism within A_r. Using $A_r = 6400$ km^2, the area over which the nonhomogeneous Poisson models were calculated in Figures 4-1a — 4-1d, it is clear that in the Crater Flat area, where most Quaternary volcanism has occurred, the probabilities of volcano formation are much higher using the near-neighbor method than indicated by the homogeneous Poisson model. As A_r decreases, the probability of volcano formation increases in the homogeneous Poisson model. If A_r decreases from 6,400 to 3,200 km^2, the probability of volcano formation in 10,000 yr and in a given 8 km^2 simply doubles to 0.6×10^{-4}. This is equal to the probability of volcanism at Northern Cone and is less than one-half the probability of volcanism at Red Cone (Crater Flat), based on the nonhomogeneous model. If A_r decreases again to 1,600 km^2, roughly the area of the AMRV (Figure 2-1), the homogeneous Poisson model indicates probabilities approximately equal to or greater than those indicated by the nonhomogeneous model.

The nonhomogeneous model better indicates the probability of volcanism in and around Crater Flat, unless A_r is sufficiently small. If, for example, the AMRV could be defined without reference to the distribution of Quaternary volcanoes, then the homogeneous model performs better through time than the nonhomogeneous model in predicting the locations of Crater Flat volcanoes. However, defining A_r to be a small region cannot be done with confidence. If A_r were chosen to be the smallest area encompassing a set of past events, as the AMRV and the CFVZ are defined, there is a high risk of failure of the homogeneous Poisson model because there is a chance future events will fall outside this zone. The

Table 4-2. Comparison of the results of nonhomogeneous (P_{nh}) and homogeneous (P_h) Poisson models

Volcano	λ_r (v/my)	A^1 $P_h \times 10^4$	A^2 $P_h \times 10^4$	A^3 $P_h \times 10^4$	$P_{nh} \times 10^4$
Lathrop Wells (1)	6.0	0.7	1.4	2.8	3.2
Sleeping Butte (2)	7.0	0.8	1.7	3.4	0.3
Crater Flat (5)					
Northern Cone	2.4	0.3	0.6	1.2	0.6
Black Cone	2.4	0.3	0.6	1.2	0.8
Red Cone	2.4	0.3	0.6	1.2	1.3
Little Cone NE	2.4	0.3	0.6	1.2	1.0
Little Cone SW	2.4	0.3	0.6	1.2	1.0
$P_h = [\,1-\exp(-\lambda_r \times 10{,}000)](A)$, where λ_r is annualized					
$A^1 = 1.25\times10^{-3}$, $A_r = 6400$ km^2					
$A^2 = 2.5\times10^{-3}$, $A_r = 3200$ km^2					
$A^3 = 5.0\times10^{-3}$, $A_r = 1600$ km^2					

nonhomogeneous model captures the essential aspects of volcano distribution in the region, without an arbitrary definition of A_r. Because cinder cones tend to form in the same area through time, this strengthens the performance of the nonhomogeneous Poisson model. Conversely, the limitations of the near-neighbor model are illustrated by the Sleeping Butte volcanoes. At Sleeping Butte, the homogeneous model indicates a higher probability of volcanism because a m=6 near-neighbor model is used in the analysis and fewer than six volcanoes are located in the Sleeping Butte area. Because comparatively few volcanoes have formed in the Sleeping Butte area, the m=6 near-neighbor model indicates that probabilities there are lower than on average throughout the region. Using fewer near neighbors increases the probability of volcanism in the Sleeping Butte area substantially, but also results in regional recurrence rates that are higher than reasonable. In a practical sense we are most interested in the performance of the models in the area of Crater Flat, because the probability of volcanism at or near Yucca Mountain is of interest.

The probability of volcanic disruption of the proposed HLW repository site calculated using near-neighbor nonhomogeneous methods is slightly higher than indicated by most calculations based on homogeneous Poisson models. For example, Crowe et al. (1982) propose a range of probability of disruption between 4.7×10^{-4} and 3.3×10^{-6} in 10,000 yr, noting that only a worst case model leads to probabilities in excess of 1×10^{-4}. Other reported ranges of between 1×10^{-6} and 1×10^{-4} in 10,000 yr (Crowe et al., 1992) do not encompass the probabilities of 1×10^{-4} to 3×10^{-4} generally calculated using the near-neighbor nonhomogeneous model (Connor and Hill, 1993). These differences arise because the candidate repository site is relatively close to the youngest large volcano cluster in the YMR. The Connor and Hill (1993) nonhomogeneous models estimate that the probability of volcanism within one repository area (8 km^2) in Crater Flat Valley is much higher, on the order of 1×10^{-3} in 10,000 yr. Probabilities of 1×10^{-3} are similar to worst case models of repository disruption in which structural controls, such as those that may have resulted in the alignment of cinder cones in Crater Flat, are assumed to focus magmatism (Smith et al., 1990; Ho, 1992).

5 AN EXAMPLE OF MODEL TESTING: SPRINGERVILLE VOLCANIC FIELD, ARIZONA

The SVF provides excellent possibilities for the evaluation of volcanism probability models and the evaluation of inaccuracy and imprecision inherent in the application of these models. The SVF:

- Is one of the best mapped cinder cone fields, having been the site of numerous, recent field investigations (Aubele et al., 1986; Condit et al., 1989; Crumpler et al., 1989; Ulrich et al., 1989; Condit, 1991).
- Has gone through a waxing, steady-state, and waning phase of activity, with the last eruption occurring at about 0.3 ± 0.1 Ma. Numerous age determinations have been made on the basalts in the SVF (Condit and Shafiqullah; 1985; Condit et al., 1989; Cooper et al., 1990). In addition to these dates, the stratigraphy of the field is well documented (Condit et al., 1994), and both numeric dates and lava flow stratigraphy can be related to individual vents.
- Contains a large number of vents distributed in a clustered pattern (Figure 5-1). Regional patterns in volcanism within the SVF, such as changes in the locus of volcanism through time and recognition of vent alignments and their relation to crustal structures, have been determined through previous investigations (Condit et al., 1989; Connor et al., 1992).

These SVF features make it an excellent analog area for the study of the behavior of probability models, with emphasis on comparison of these models and uncertainty associated with their use. However, the SVF is part of the Colorado Plateau volcanic system, which is a distinct tectonic setting from the YMR. As such, the results of these probability models such as cluster intensity or volcano recurrence rates cannot be directly applied to the YMR.

5.1 VOLCANO AGES FOR THE SRINGERVILLE VOLCANIC FIELD

Available K-Ar dates for lava flows in the SVF are summarized in Table 5-1. These 36 dates represent approximately 10 percent of the SVF and are used to bound the ages of other lava flows and vents. The possible age ranges of 329 of the remaining undated lava flows can be inferred through stratigraphic relationships with dated flows. For example, a lava flow sequence of ten cooling units may lie stratigraphically between two dated flows. Obviously, these ten cooling units must have formed between the times of deposition of the two dated flows. These ranges are further constrained, in many cases, by paleomagnetic data (Condit et al., 1989). It is assumed that the undated flows have ages that are distributed according to a uniform random distribution over the interval bounded by the dated flows and/or magnetic polarity reversals, including uncertainties in the K-Ar dates. In other words, there is an equal probability of a vent forming early, late, or in the middle of the age range defined by the dated samples, with the expected age being the average age of the two numerically dated flows. A confidence interval for the age of each cooling unit and vent was established in this manner. The ages of 44 vents in the field have not been estimated by these techniques. These vents are located at the south-central margin of the field on Navajo reservation land; access to these vents and lava flows for the purposes of sampling has been denied by reservation authorities, and, as a result, age estimates have not been made.[1]

[1](C.D. Condit, pers. comm. to C.B. Connor, 1993).

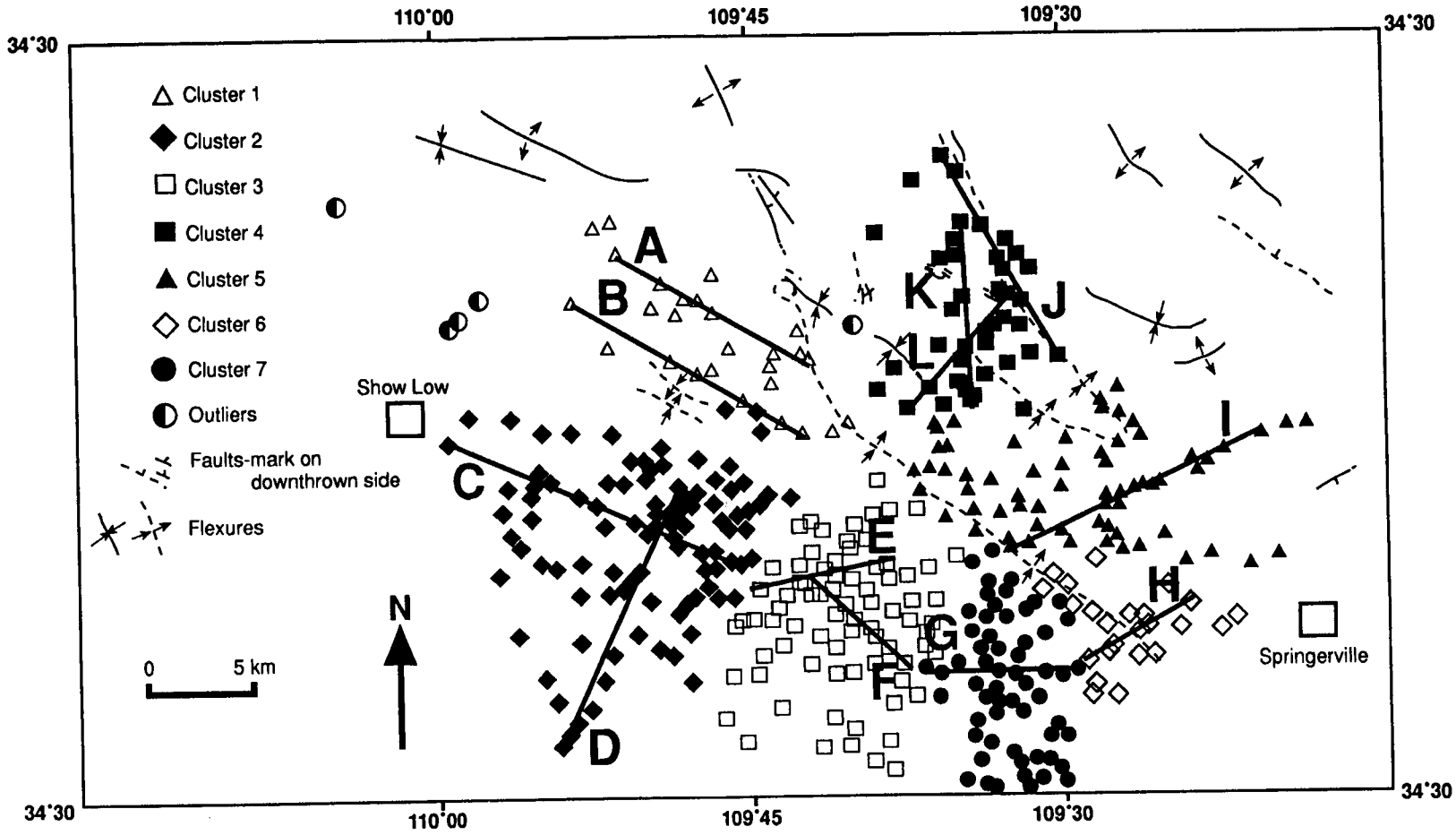

Figure 5-1. Vents in the Springerville Volcanic Field plotted by cluster (Connor et al., 1992). Vent alignments, identified through statistical analysis, are labeled A-L. Mapped faults and flexures also are shown.

Table 5-1. Dates for volcanic lavas and cinder cones of the Springerville Volcanic Field, Arizona. Error represents reported 1-sigma uncertainty associated with the date.

Sample	Unit	Date (Ma)	Error (Ma)	Source
705MC'	Qhe	0.50	0.03	Cooper and others, 1990
706GP'	Qph2	1.27	0.07	Cooper and others, 1990
708WK'	Qgh7	0.76	0.02	Cooper and others, 1990
709WK'	Qgbl	0.91	0.02	Cooper and others, 1990
712GP'	Qpc8	1.30	0.04	Cooper and others, 1990
716SM'	Qmb6	1.01	0.02	Cooper and others, 1990
719V'	Qvc4	1.00	0.02	Cooper and others, 1990
801C'	Tof	6.52	0.12	Cooper and others, 1990
801C"	Tof	6.66	0.12	Cooper and others, 1990
2316-2	Twj	7.6	0.4	Miller, oral commun., 1991
AWL-40-74	Trg	2.94	0.14	Laughlin and others, 1979
AWL-41-74	Qrg	0.82	0.04	Laughlin and others, 1979
AWL-42-74	Tacl	3.06	0.08	Laughlin and others, 1979
AWL4-77	Qdh4	0.84	0.07	Laughlin and others, 1979
AWL5-77	Qag	1.67	0.09	Laughlin and others, 1979
AWL6-77	Qkc6	0.75	0.13	Laughlin and others, 1979
UAKA 73-80	QTsf	1.62	0.08	Peirce and others, 1979
UAKA 73-137	QTsf	1.63	0.08	Peirce and others, 1979
UAKA 74-136	QTsf	1.90	0.06	Peirce and others, 1979
UAKA 75-52a	QTsf	1.76	0.15	Peirce and others, 1979
UAKA 80-131	Qsc5	1.53	0.21	Condit and Shafiqullah, 1985
UAKA 80-132	Qsg2	1.74	0.15	Condit and Shafiqullah, 1985
UAKA 80-133	QTsf	1.78	0.22	Condit and Shafiqullah, 1985
UAKA 80-134	Tbc3	1.83	0.21	Condit and Shafiqullah, 1985
UAKA 80-135	Tbl	8.66	0.19	Condit and Shafiqullah, 1985
UAKA 80-136	Tbcl	8.97	0.19	Condit and Shafiqullah, 1985

Sample	Unit	Date (Ma)	Error (Ma)	Source
UAKA 82-95	Tnc	2.05	0.10	Condit and Shafiqullah, 1985
UAKA 82-96	Qnd	1.47	0.06	Condit and Shafiqullah, 1985
UAKA 82-183	Qbb2	1.65	0.09	Condit and Shafiqullah, 1985
UAKA 82-184	Qme	0.49	0.03	Condit and Shafiqullah, 1985
UAKA 82-185	QTsf	2.00	0.11	Condit and Shafiqullah, 1985
UAKA 82-190	Qek	1.56	0.05	Aubele and others, 1986
UAKA 82-191	Qvc4	1.30	0.05	Aubele and others, 1986
UAKA 82-192	Qcb1	1.19	0.04	Aubele and others, 1986
UAKA 82-193	Qde3	1.05	0.04	Aubele and others, 1986
UAKA 82-195	Qkb2	0.31	0.07	Aubele and others, 1986
UAKA 82-196	Quh4	1.04	0.05	Aubele and others, 1986
UAKA 82-197	Qgj2	0.67	0.02	Aubele and others, 1986

One way to represent the temporal pattern of volcanism in the SVF is by plotting the cumulative number of vents through time (Figure 5-2a). Vent age determinations were averaged at 0.25-Ma intervals using expected, minimum, and maximum vent ages for the 365 vents for which age estimates are available. This time interval, 0.25 Ma, was chosen because separation of the data into shorter time intervals is not warranted, given the uncertainty in the age estimates. Despite the uncertainty in the ages, it is clear that the SVF, as a whole, has gone through a waxing stage of activity prior to about 2 Ma, a steady-state phase in which the numbers of vents formed were relatively constant, and finally a waning stage. After about 1.0 Ma, the number of vents formed decreased dramatically. The youngest vents in the SVF are approximately 0.3 Ma.

An alternate way to look at these data is to plot the number of vents that may have formed in a given 0.25-Ma interval (Figure 5-2b). On lavas with age determinations, the precision of the age determinations is taken into account and the lava can be assigned to the given interval with greater than 84 percent confidence. These dated lavas stratigraphically bound undated lavas, which therefore have ages that are between dated lavas; the probability that these undated lavas belong to a given interval is determined assuming that the ages of the lavas has a uniform random distribution, bounded by the dated lavas. Errors shown in Figure 5-2b look worse than those in Figure 5-2a because the data are not treated cumulatively. For example, it is possible that almost 200 vents formed in the intervals between 1.5 and 1.75 Ma, and between 1.25 and 1.5 Ma; but both cannot be true. It is important to keep this imprecision in age determinations in mind throughout the analysis. The main comparison is between the uncertainty in the application of the probability model, for instance in the determination of the number of near-neighbor vents to use, and the uncertainty in the age determinations.

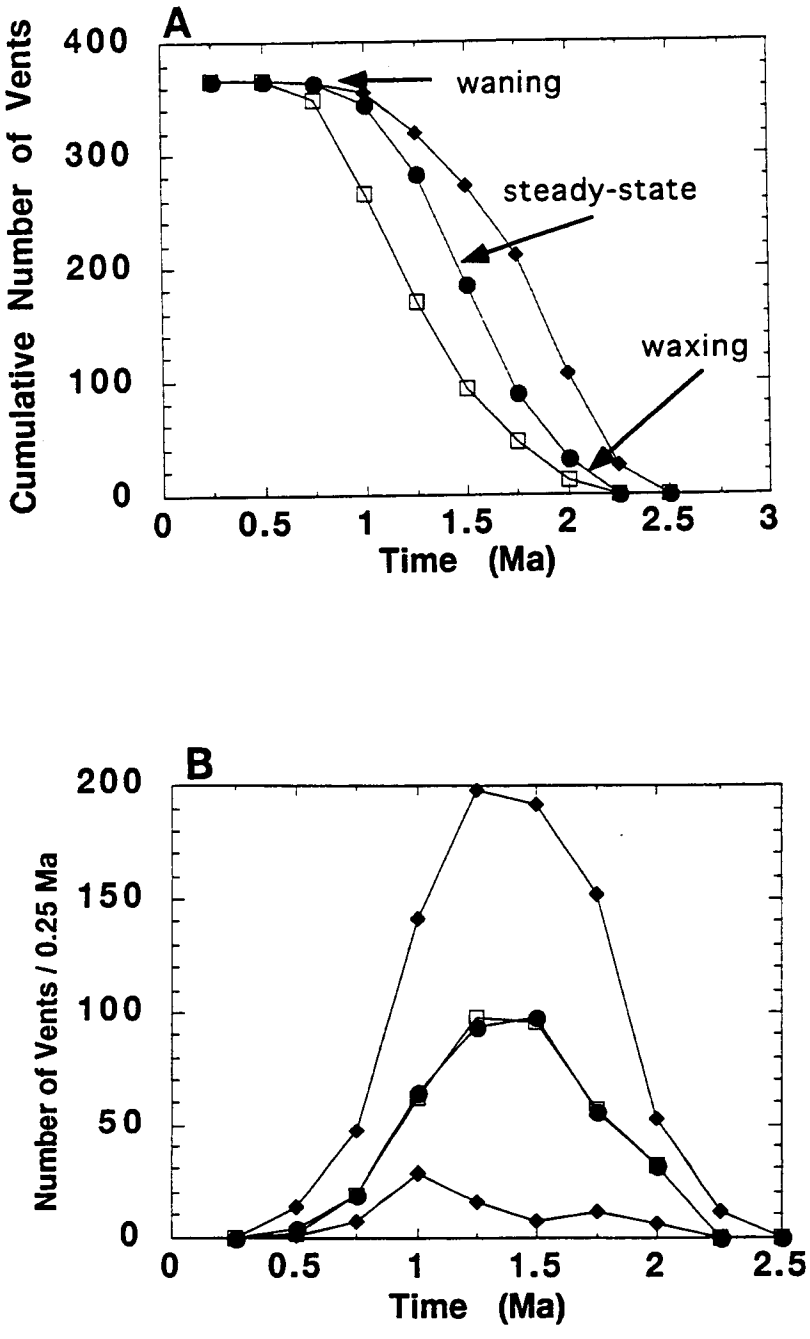

Figure 5-2. (a) Cumulative number of vents determined using mean expected ages, maximum, and minimum ages for individual vents. (b) The number of vents formed in a given interval with 84 percent confidence. Line with solid circle shows the expected number of vents per interval, lines with solid diamond correspond to the 84 percent confidence envelope, line with the open squares uses best-guess ages, which are sometimes different than the expected number of vents, based on additional geologic information (Condit et al., 1994).

Scatter plots of the distribution of vents by time interval (Figures 5-3a and 5-3b) give an indication of the importance of spatial variation in the distribution of vents within the SVF through time. For example, the distribution of vents thought to have formed between 1.25 and 1.0 Ma, near the height of volcanic activity (Figure 5-2b), is shown in Figure 5-3a. Vents formed during this period are widely distributed. However, three clusters of vents in the southern part of the field were especially active during this interval. Activity decreased most dramatically in the western part of the field during the next 0.25 my, and an ENE-trending vent alignment developed in the eastern part of the field (Figure 5-3b).

These are the basic data available from the SVF for evaluation and comparison of probability models. It seems appropriate that probability models should capture the temporal variation in recurrence rate in the SVF (Figures 5-2a and 5-2b) and the spatial variation in recurrence rate (Figures 5-3a and 5-3b).

5.2 ESTIMATING RECURRENCE RATES IN THE SPRINGERVILLE VOLCANIC FIELD

Recurrence rate was estimated using Eqs. (3-4) to (3-6) and various numbers of near-neighbor vents. Summarizing the analysis, the first step is to determine the distance from the point at which the recurrence rate is to be estimated, (x,y), to each volcano in the field. This distance becomes the radius of a circle of area, u_i, where i refers to the ith volcano. The area u_i is multiplied by the age of the volcano, t_i, or the difference between the age of the volcano and the time of the recurrence-rate calculation. The values of $u_i t_i$ are then sorted in ascending order. The closest near-neighbor is closest in terms of time and distance. The second near neighbor is a little further away, or perhaps a little closer spatially but is older than the nearest neighbor. A total of m near-neighbors is then used to estimate the recurrence rate at (x,y). If fewer near-neighbors are used, then the recurrence rate will be comparatively high because only the closest vents are used. Using more near-neighbors averages in more distant and/or older vents and the recurrence rate decreases. One approach in estimating the number of near-neighbor vents to use is integrate the estimates across the entire region [Eq. (3-6)]. The resulting values then can be compared with other estimates of the regional recurrence rate (Connor and Hill, 1993). In the case of the SVF, where age estimates on a large number of vents have been made, it is also possible to compare estimates of the regional recurrence rate through time (Figure 5-2b).

Calculations were made using $m=6,7,8$, and 10 near-neighbor vents and Eqs. (3-4) to (3-6). The results of these calculations were compared with the regional recurrence rate (Figure 5-4). Calculations were made at 0.25-Ma intervals, using only vents erupted prior to the time of the calculation in order to compare the near-neighbor estimates directly with the age data. Overall, the near-neighbor models track the variation in estimated recurrence rate well, increasing before 1.25 Ma, and decreasing after 1.0 Ma. The $m=7$ and 8 near-neighbor models are the mean estimated recurrence rate before 1.0 Ma, when the system is waxing or steady. The near-neighbor models predict a more rapid decrease in activity before 0.75 Ma than actually occurred. As a result, the $m=6$ near-neighbor model best matches the mean estimated recurrence rate best over this interval (Figure 5-4). However, comparison with Figure 5-2b indicates that all of these near-neighbor models are within the range of estimates for volcanism recurrence rate.

After 0.75 Ma, the near-neighbor models overestimate the recurrence rate compared with the mean estimated recurrence rate. This is, in part, due to the nature of the estimation technique. Volcanism does not occur in the field after 0.3 Ma, but using Eq. (3-4), the recurrence-rate estimate cannot decrease

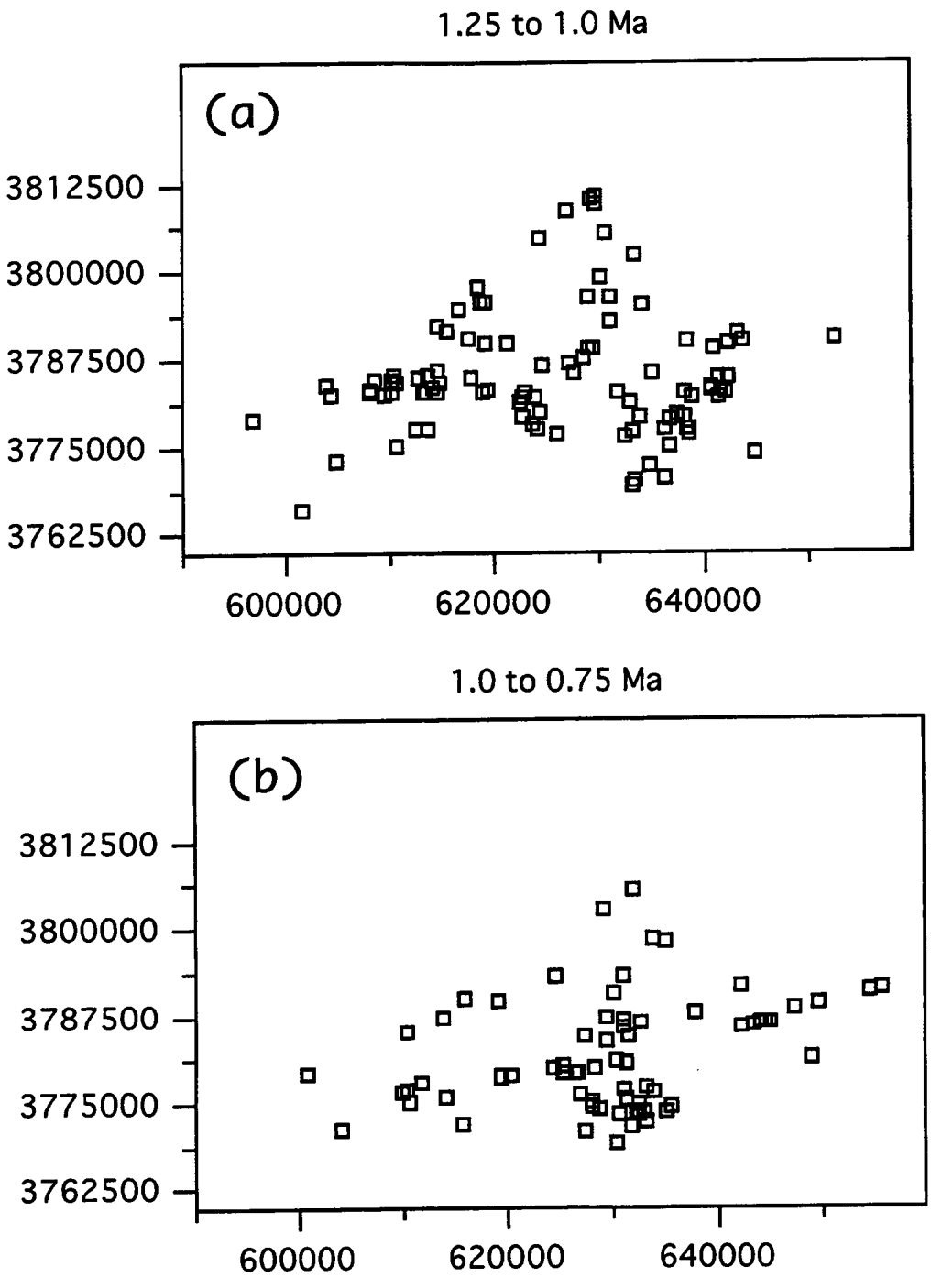

Figure 5-3. Scatter plots of vents thought to have formed between (a) 1.25 and 1.0 Ma, and (b) 1.0 and 0.75 Ma. Note the change in vent distribution with time. Axis coordinates are in Universal Transverse Mercator.

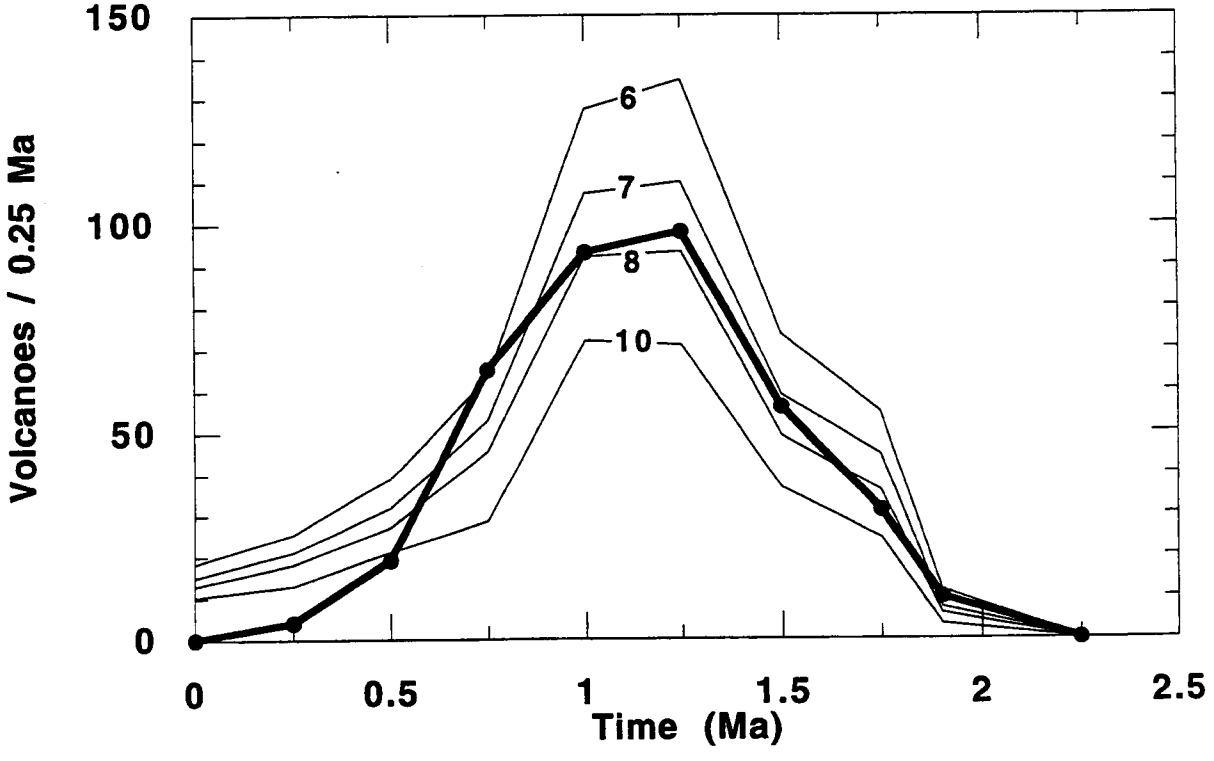

Figure 5-4. Comparison of estimates of recurrence rate based on different near-neighbor models (labeled lines) and the observed, mean estimate of recurrence rate (heavy line with solid circles), calculated at 0.25 my intervals. The $m=7$ and 8 near-neighbor models accurately reflect estimated recurrence rate before 1.0 Ma, although all models work well with respect to the uncertainty in the age determinations.

to zero. This suggests that in fields with waning volcanic activity, the near-neighbor estimation techniques have a tendency to overestimate the recurrence rate. In a field where magmatism clearly is waning, such as the SVF, the near-neighbor estimates of recurrence rate can be modified. Rather than including all volcanoes formed prior to the time of the calculation, it is possible to include only those volcanoes formed during an interval of time, such as 0.5 my, prior to the time for which the calculation is made. For example, making an estimate of recurrence rate for the SVF at 1.0 Ma, one might only include volcanoes formed between 1.5 Ma and 1.0 Ma in the calculation. This modification effectively suggests that a large volcanic field, such as the SVF, has a limit to the memory of the system. In essence, it may make no difference what volcanic activity was like at 1.0 Ma; only the geologically recent past (i.e., 0.5 Ma) provides an indication of future activity. Such a finding supports the application of non-Poissonian models, such as spatio-temporal Markov models, in which system memory can be incorporated directly. Such an assumption may have a geophysical basis, for instance, in the duration of heat flow anomalies (e.g., Marsh, 1984). Figure 5-5 shows a comparison of the observed change in recurrence rate and $m=7$ and 8 near-neighbors, using 0.5-Ma intervals. Both near-neighbor models capture the decrease in volcanism after 0.5 Ma much better than previous calculations. As before, both models slightly underestimate the recurrence rate at 0.75 Ma in the observed data. These types of perturbations occur because of clustering of vent ages within the time interval, relative to the time of the calculation. Given the relatively low resolution of the data, it is not possible to determine if these perturbations actually occurred within the field.

The impact of changing the length of the time interval in the near-neighbor models can be assessed also. The $m=7$ near-neighbor recurrence rate was calculated using an interval of 2 Ma, essentially using the entire data set, 0.5 Ma, as above, and 0.25 Ma (Figure 5-6). The 0.25-Ma interval tends to underestimate recurrence rate during the last 1.0 Ma. Similar techniques can be applied to Weibull-Poisson estimates of recurrence rate. This will provide some sense of the impact of uncertainty in parameters, particularly t [(Eqs. (3-1) to 3-3)], on probability estimates of volcanic events.

These nearest-neighbor estimation techniques are important because they provide a basis for mapping the local recurrence rate across the SVF. Scatter plots of vents formed in 0.25-Ma intervals in the SVF (Figures 5-3a and 5-3b) indicate that significant shifts in volcano locations occur within the field. Spatial variation in recurrence rate is mapped by time interval, in this case using $m=7$ near neighbors. The variation in the recurrence rate of volcanism is shown in Figure 5-7, and the change in the recurrence rate of volcanism is shown in Figure 5-8. The change in recurrence rate through time is calculated by differencing two recurrence-rate maps. For example, to find the change in the recurrence rate through time between 1.25 Ma and 1 Ma, the 1.25-Ma data is subtracted from the 1.0-Ma map. Figure 5-8 is particularly useful because it illustrates area where volcanism is developing (i.e., waxing) most clearly. Dark areas show where volcanism is waning the most rapidly; and red areas show where it is steady through time, including parts of the field where no volcanism is occurring at all.

Specific areas are most active at certain times in the SVF (Figure 5-8) and can be related to spatial clusters in the field (Figure 5-1) (Connor et al., 1992). Such correlations indicate a geological basis for spatial patterns in vent distribution. These patterns may correspond to specific zones of melt generation or a higher degree of magma production at a particular time, and therefore can be compared directly with petrologic data. As probability models continue to develop and incorporate geologic information, the results of these models can be directly compared to other geologic data such as geochemical characteristics. This comparison will provide a solid empirical basis for linking probability model results to geologic processes.

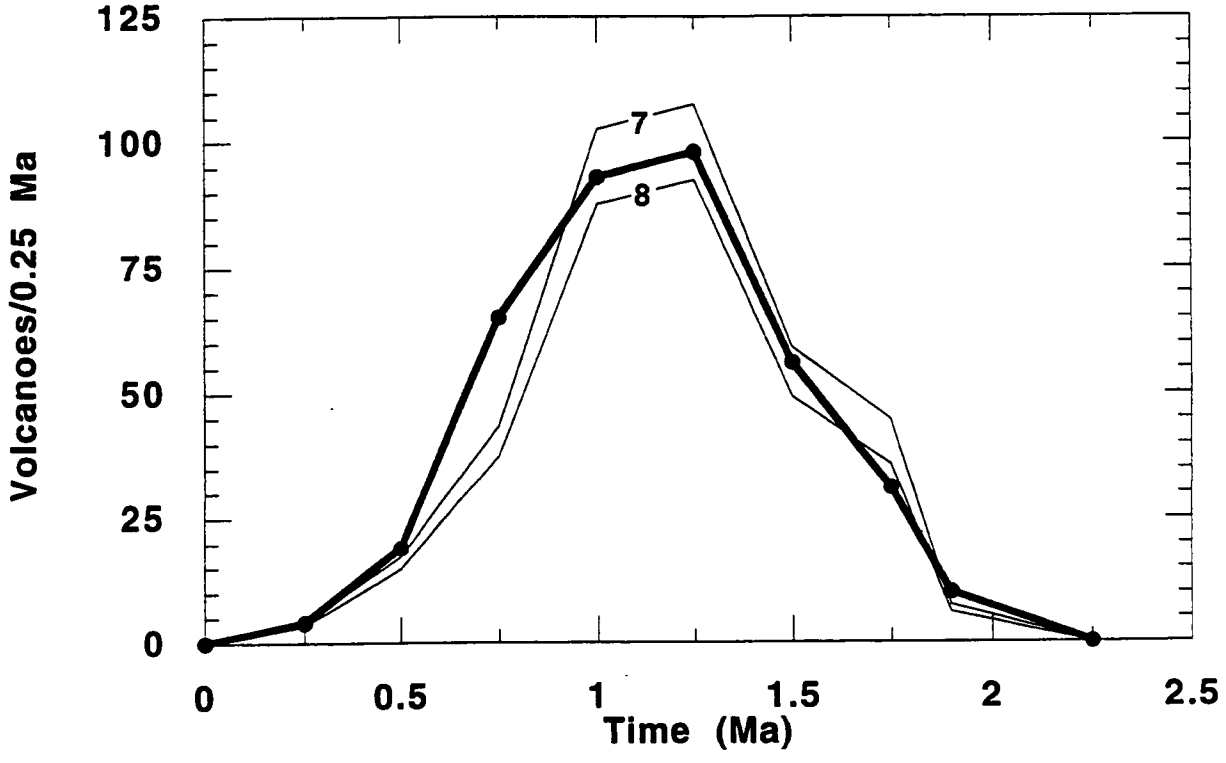

Figure 5-5. Volcanism is waning in the SVF; no eruption has occurred in the field within approximately the last 0.3 my This waning is captured by the near-neighbor models if estimates are made using 0.5-Ma intervals, rather than all of the volcanoes formed prior to the time for which the calculation is made. Near-neighbor models $m=7$ and 8 are shown. The mean estimated recurrence rate based on age determinations is shown by the heavy solid line with solid circles).

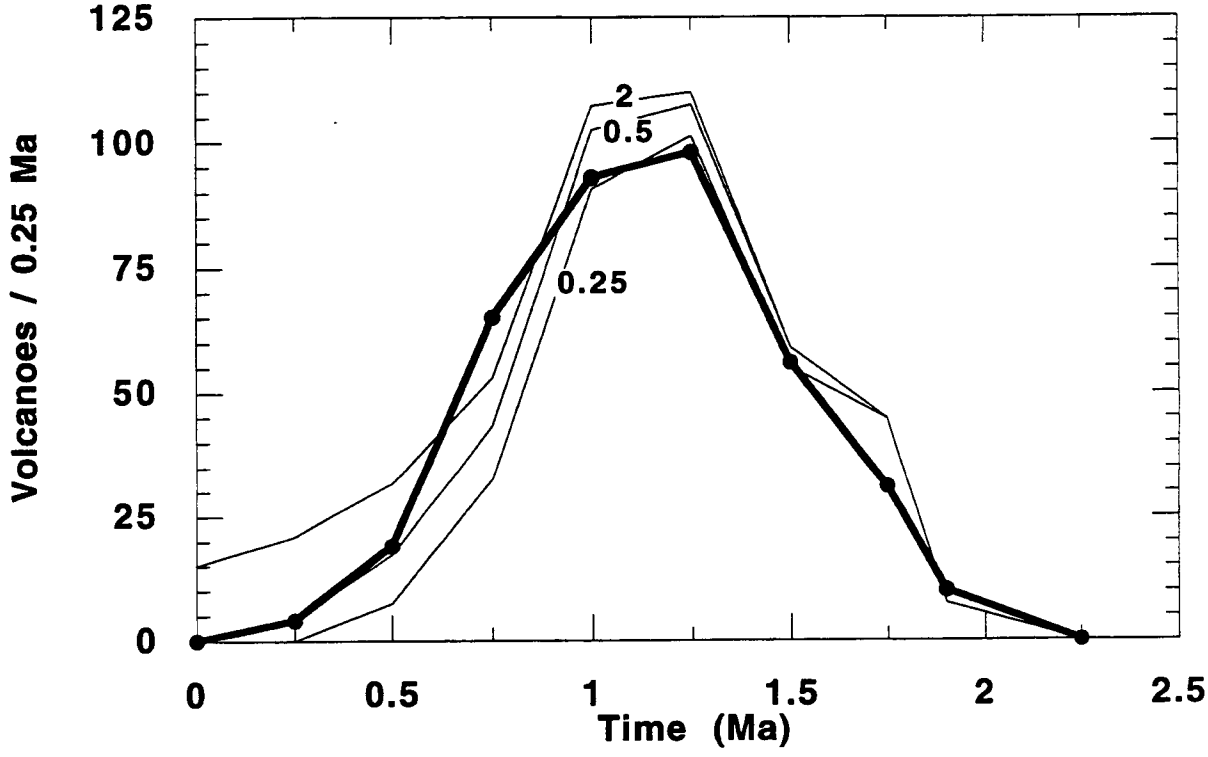

Figure 5-6. Comparison of the $m=7$ near-neighbor models calculated using intervals of 0.25, 0.5, and 2 my. The 0.5-Ma interval model most closely matches the change in the observed data. The mean estimated recurrence rate based on age determinations is shown by the heavy solid line with solid circles.

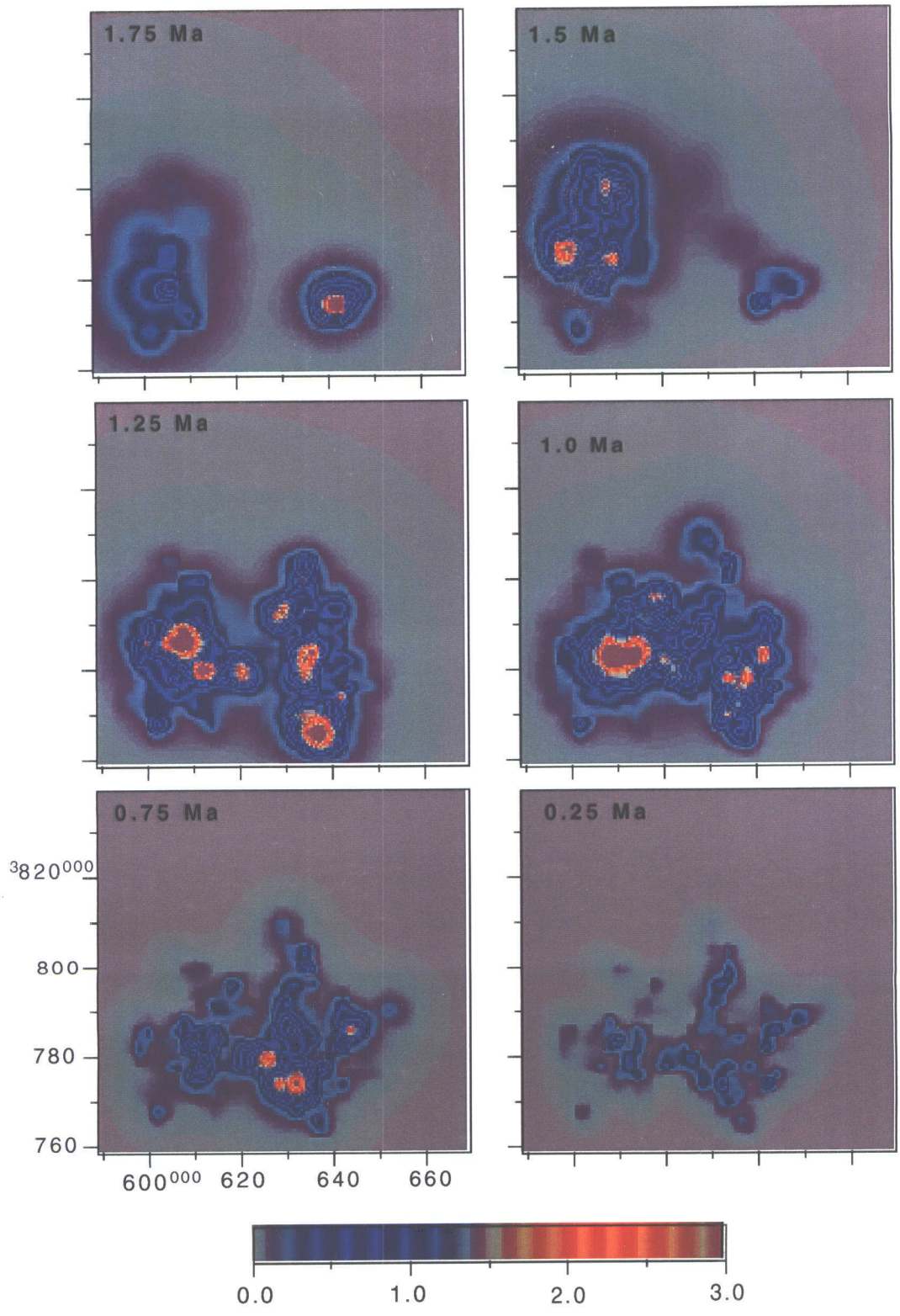

Figure 5-7. Variation in recurrence rate for the Springerville Volcanic Field using an *m*=7 near-neighbor model and 0.25-Ma intervals of time. Contours are in v/0.25 Ma.

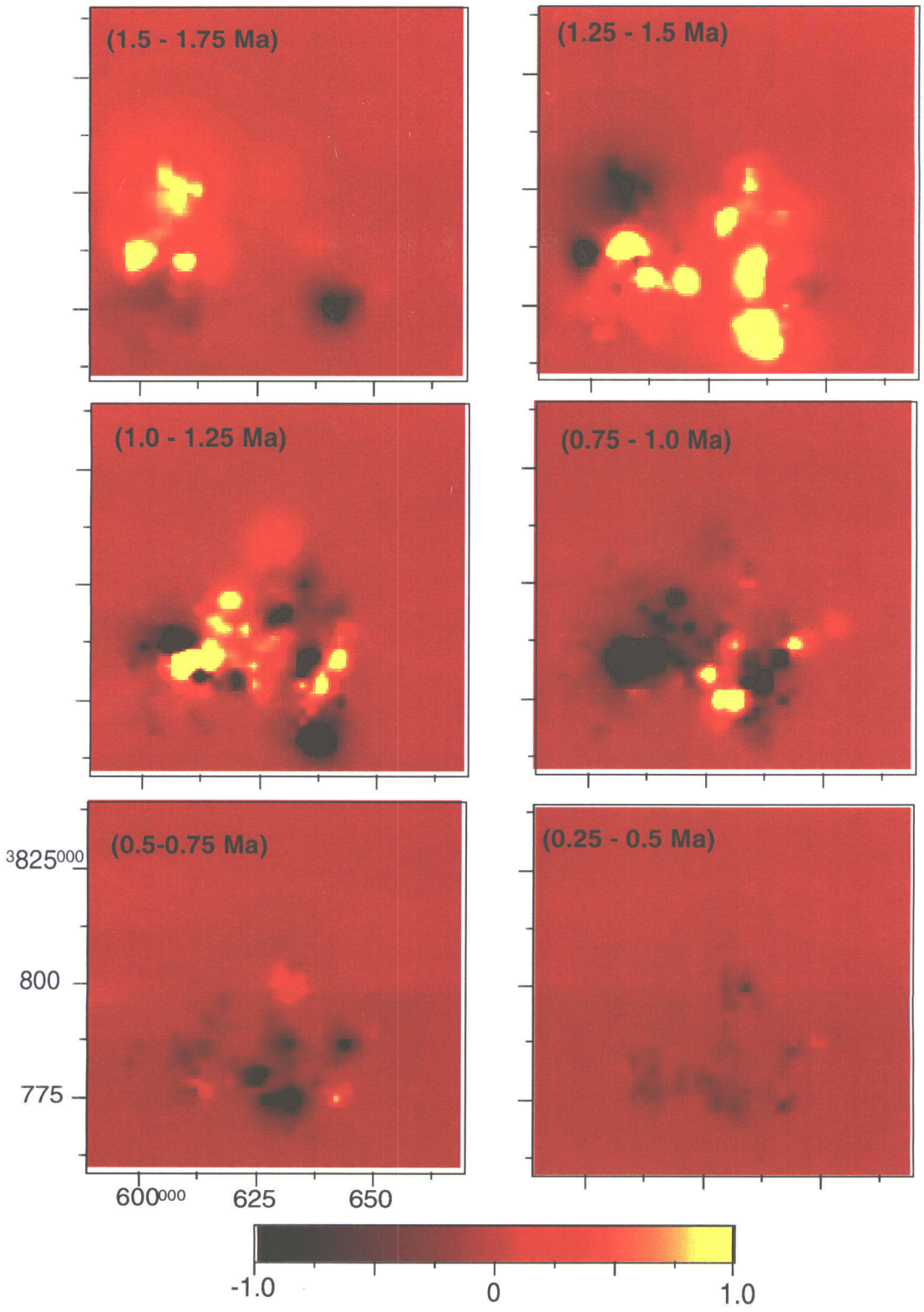

Figure 5-8. Relative changes in recurrence rate for the Springerville Volcanic Field using an *m*=7 near-neighbor model and 0.25-Ma intervals of time. Shading represents change in recurrence rate from preceding 0.25-Ma interval. Yellow areas represent zones of waxing volcanism, darker areas are zones of waning volcanism.

6 SUMMARY AND RECOMMENDATIONS

Although there are numerous models for the probability of volcanic disruption of the candidate HLW repository at Yucca Mountain, there is currently no objective or quantitative procedure to evaluate the precision and accuracy of these models. Published probabilities of volcanic disruption of the candidate repository during the next 10,000 yr range from 10^{-6} (e.g., Crowe et al., 1982, 1992) to 10^{-3} (e.g., Ho et al., 1991). These probability models will need to be evaluated as part of the HLW repository licensing review.

The uncertainties associated with volcanism probability models have yet to be addressed in detail and are rarely even quantified. These uncertainties can be generally characterized as errors associated with the precision of basic model data, and the accuracy of probability models to reproduce observed volcanologic processes. Data and assumptions used in these models clearly have associated uncertainties, which can range from negligible to very large. Although uncertainty can be minimized for some model parameters, it cannot be eliminated and thus must be propagated through probability calculations. Realistic comparisons of model results also cannot be achieved until the same basic geologic data and uncertainties are utilized in the different models.

In addition to the quantification of uncertainties associated with basic geologic data, probability models also must be tested for accuracy. These tests can be accomplished by evaluating how well models predict the location of volcanoes through time in the YMR. Because there are relatively few volcanoes in the YMR, probability models also must be tested in other analogous volcanic fields. Although the analog fields have important differences in their volcanic environments, they contain more volcanoes and generally exhibit more spatial and temporal variations than the YMR volcanoes. Therefore, analogs provide a means of testing models with regard to their sensitivity to assumptions and estimated parameters.

Therefore, a recommended strategic approach to probability model evaluation occurs in the following general sequence:

- Evaluation of the fundamental geologic assumptions used in the models, including selection of time intervals, areas, and parameters
- Quantification of the precision associated with the basic geologic data used in the models; basic data include age determinations and volume estimates
- Application of the same basic data to the individual probability models
- Calculation of confidence intervals for probability models to evaluate the significance of differences between conceptually distinct probability models
- Application of the models to different periods of time in the YMR to evaluate models in reproducing the observed spatial and temporal patterns of volcanic activity
- Evaluation of model sensitivities to variations in tectonic and volcanic processes that occur between the YMR and analog volcanic fields

- Application of the models to appropriate YMR-analogous volcanic fields to further evaluate model accuracy in reproducing known spatial and temporal patterns of volcanic activity

Model evaluation is predicated on numerous basic data requirements. Primarily, uncertainties in model data must be quantified and reported. Parameters such as eruptive volume, number and location of vents, and volcano age all have associated uncertainties that must be rigorously propagated through ensuing calculations. If these uncertainties are not reported by individual researchers, then they must be estimated using reasonable assumptions of the precision and accuracy of the analytical technique. In addition, nonaveraged data must be reported to ensure that appropriate uncertainties are associated with averaged values. Calculated standard deviations of small data sets rarely represent the uncertainty in the average, when large (e.g., >20 percent) errors are associated with the data.

The number, location, and age of volcanic centers in the YMR remains controversial (Crowe et al., 1982, 1993; Smith et al., 1990; Connor and Hill, 1993). It is thus imperative that these parameters are reported with all probability models so that conceptual differences in these models can be distinguished from simple differences in basic YMR volcanic data.

No volcanic fields are completely analogous to the YMR. Potentially significant variations in magma production and eruption rates, local and regional tectonic setting, and crustal structure likely affect spatial and temporal patterns of volcanism at analogous areas. However, probability models may be relatively insensitive to these variations. These variations must be addressed, because the YMR does not contain a sufficient number of volcanoes to robustly test probability model performance. Based on the evaluation of data available from the Volcanic Systems of the Basin and Range research project, proposed analogs for probability model testing are the CFV and CoVF of California, and the SVF of Arizona. The analog volcanic fields are relatively well studied and often have clear spatial and temporal patterns of volcanic processes.

Finally, probability model evaluation needs to remain strongly integrated with ongoing volcanism and PA research programs. Probability model development and compilation of data for analog volcanic fields are continuing tasks in the Volcanic Systems of the Basin and Range research project. The evaluation of data precision and accuracy also is ongoing in this project. Basic geologic data used in probability models, such as the area of disruption associated with mafic volcanic eruptions, are being collected as part of the Field Volcanism research project. Resulting probability models need to be incorporated into PA research to evaluate the significance of different volcanism probabilities on repository performance. Although current probabilities of volcanic disruption at times appear similar, most of these models have yet to be evaluated in detail.

7 REFERENCES

Armstrong, R.L., and P. Ward. 1991. Evolving geographic patterns of Cenozoic magmatism in the North American Cordillera: The temporal and spatial association of magmatism and metamorphic core complexes. *Journal of Geophysical Research* 96: 13,201-13,224.

Aubele, J.C., L.S. Crumpler, M. Shafiqullah. 1986. K-Ar ages of late Cenozoic rocks of the central and eastern parts of the Springerville Volcanic Field, east-central Arizona. *Isochron/West* 46: 3-5.

Bacon, C.R. 1982. Time-predictable bimodal volcanism in the Coso Range, California. *Geology* 10: 65-69.

Barca, R.A. 1965. *Geologic Map and Sections of the Northern Portion of the Old Dad Mountain Quadrangle, San Bernardino County, California.* California Division of Mines and Geology Map Sheet 7. Sacramento, CA: California Division of Mines and Geology.

Breslin, P.A. 1982. *Geology and Geochemistry of a Young Cinder Cone in the Cima Volcanic Field, Eastern Mojave Desert, California.* M.S. Thesis. Los Angeles, CA: University of California.

Christiansen, R.L., and P. Lipman. 1972. Cenozoic volcanism and plate tectonic evolution of the western United States: II, Late Cenozoic. *Philosophical Transactions of the Royal Society of London* A-271: 249-284.

Condit, C.D. 1984. *Geology of the Western Part of the Springerville Volcanic Field, East-Central Arizona.* Ph.D. Thesis. Albuquerque, NM: University of New Mexico.

Condit, C.D. 1991. *Lithologic Map of the Western Part of the Springerville Volcanic Field, East-Central Arizona.* U.S. Geological Survey Miscellaneous Investigations Series Map I-1993, scale 1:50,000. Reston, VA: U.S. Geological Survey.

Condit, C.D., and M. Shafiqullah. 1985. K-Ar ages of late Cenozoic rocks of the western part of the Springerville Volcanic Field, east-central Arizona. *Isochron/West* 44: 3-5.

Condit, C.D., L.S. Crumpler, J.C. Aubele, and W.E. Elston. 1989. Patterns of volcanism along the southern margin of the Colorado Plateau: The Springerville Field. *Journal of Geophysical Research* 94(B6): 7,975-7,986.

Condit, C.D., L.S. Crumpler, and J.C. Aubele. 1994. *Thematic Geologic Maps of Parts of the Springerville Volcanic Field, East-Central Arizona.* U.S. Geological Survey Miscellaneous Investigations Series Map, in review. Reston, VA: U.S. Geological Survey.

Connor, C.B. 1993. *Technical and Regulatory Basis for the Study of Recently Active Cinder Cones.* IM-20-5704-141-001. San Antonio, TX: Center for Nuclear Waste Regulatory Analyses.

Connor, C.B. 1994. *Status of CNWRA Volcanological Probability Studies*. Presentation to the Nuclear Waste Technical Review Board, Panel on Structural Geology and Geoengineering. Meeting on Probabilistic Seismic and Volcanic Hazard Estimation. Bethesda, MD: Nuclear Waste Technical Review Board.

Connor, C.B., and B.E. Hill. 1993. Estimating the probability of volcanic disruption of the candidate Yucca Mountain repository using spatially and temporally nonhomogeneous poisson models. *Proceedings, American Nuclear Society Focus '93 Meeting*. La Grange Park, IL: American Nuclear Society 174–181.

Connor, C.B., and B.E. Hill. 1994. *The CNWRA Volcanism Geographic Information System Database*. CNWRA 94-004. San Antonio, TX: Center for Nuclear Waste Regulatory Analyses.

Connor, C.B., and C.O. Sanders. 1994. *Geophysical Topical Report: Application of Seismic Tomographic and Magnetic Methods to Issues in Basaltic Volcanism*. CNWRA 94-013. San Antonio, TX: Center for Nuclear Waste Regulatory Analyses.

Connor, C.B., C.D. Condit, L.S. Crumpler, and J.C. Aubele. 1992. Evidence of regional structural controls on vent distribution: Springerville Volcanic Field, Arizona, *Journal of Geophysical Research* 97: 12,349–12,359.

Cooper, J.L., J.L. Aronson, C.D. Condit, and W.K. Hart. 1990. New K-Ar ages of lavas from the Colorado Plateau–Basin and Range transition zone, east-central Arizona. *Isochron/West* 55: 28–31.

Coppersmith, K. 1994. *Use of Expert Judgment in Yucca Mountain Probabilistic Volcanic Hazard Assessment*. Presentation to the Nuclear Waste Technical Review Board, Panel on Structural Geology and Geoengineering. Meeting on Probabilistic Seismic and Volcanic Hazard Estimation. San Francisco, CA.

Cornell, A. 1994. *Probabilistic Natural Hazard Estimation for Use in Design of Engineered Facilities*. Presentation to the Nuclear Waste Technical Review Board, Panel on Structural Geology and Geoengineering. Meeting on Probabilistic Seismic and Volcanic Hazard Estimation. San Francisco, CA.

Cressie, N.A.C. 1991. *Statistics for Spatial Data*. New York, NY: John Wiley and Sons.

Crow, L.H. 1982. Confidence interval procedures for the Weibull process with applications to reliability growth. *Technometrics* 24: 67–71.

Crowe, B.M. 1990. Basaltic Volcanic Episodes of the Yucca Mountain Region. *High-Level Radioactive Waste Management, International Conference. April 8–12, 1990, Las Vegas, NV*. American Nuclear Society 1: 65–73.

Crowe, B.M. 1994. *Probabilistic Volcanic Risk Assessment*. Presentation to the Nuclear Waste Technical Review Board, Panel on Structural Geology and Geoengineering. Meeting on Probabilistic Seismic and Volcanic Hazard Estimation. San Francisco, CA.

Crowe, B.M., and F.V. Perry. 1989. Volcanic probability calculations for the Yucca Mountain site: Estimation of volcanic rates. *Proceedings Nuclear Waste Isolation in the Unsaturated Zone, Focus '89*. La Grange, IL. American Nuclear Society 326–334.

Crowe, B., and F. Perry. 1991. *Preliminary Geologic Map of the Sleeping Butte Volcanic Centers*. Report LA-12101-MS. Los Alamos, NM: Los Alamos National Laboratory.

Crowe, B.M., M.E. Johnson, and R.J. Beckman. 1982. Calculation of the probability of volcanic disruption of a high-level nuclear waste repository within southern Nevada, USA. *Radioactive Waste Management and the Nuclear Fuel Cycle* 3: 167–190.

Crowe, B.M., R. Picard, G. Valentine, and F.V. Perry. 1992. Recurrence models for volcanic events: applications to volcanic risk assessment. *Third Conference on Radioactive Waste Management*. Las Vegas, NV: American Nuclear Society 2: 2,344–2,355.

Crowe, B.M., F.V. Perry, and G.A. Valentine. 1993. *Preliminary Draft: Status of Volcanic Hazard Studies for the Yucca Mountain Site Characterization Project*. Los Alamos, NM: Los Alamos National Laboratory.

Crumpler, L.S., J.C. Aubele, and C.D. Condit. 1989. Influence of Quaternary tectonic deformation on volcanism in the Springerville Volcanic Field, Colorado Plateau, USA. *New Mexico Bureau of Mines and Mineral Resources Bulletin* 131: 64.

Dohrenwend, J.C., L.D. McFadden, B.D. Turrin, and S.G. Wells. 1984. K-Ar dating of the Cima Volcanic Field, eastern Mojave Desert, California: Late Cenozoic volcanic history and landscape evolution. *Geology* 12: 163–167.

Dohrenwend, J.C., S.G. Wells, and B.D. Turrin. 1986. Degradation of Quaternary cinder cones in the Cima Volcanic Field, Mojave Desert, California. *Geological Society of America Bulletin* 97: 421–427.

Dorn, R.I., J.B. Bamforth, T.A. Cahill, J.C. Dohrenwend, B.D. Turrin, D.J. Donahue, A.J.T. Jull, A. Long, M.E. Macko, E.B. Weil, D.S. Whitley, and T.H. Zabel. 1986. Cation-ratio and accelerator radiocarbon dating of rock varnish on Mojave artifacts and landforms. *Science* 231: 830–833.

Duffield, W.A., and G.R. Roquemore. 1988. Late Cenozoic volcanism and tectonism in the Coso Range area, California. *This Extended Land: Geological Journeys in the Southern Basin and Range*. D.L. Weide and M.L. Farber, eds. Geological Society of America, Cordilleran Section Field Trip Guidebook. Las Vegas, NV: University of Nevada: 159–176.

Duffield, W.A., C.R. Bacon, and G.B. Dalrymple. 1980. Late Cenozoic volcanism, geochronology, and structure of the Coso Range, Inyo County, California. *Journal of Geophysical Research* 85(B5): 2,381–2,404.

Farmer, G.L., H.G. Wilshire, J.L. Wooden, A.F. Glazner, and M. Katz. 1991. Temporal variations in the sources of alkali basalts at the Cima volcanic field, SE California. *Geological Society of America Abstracts with Programs* 23(2): 23.

Hewitt, D.G. 1956. *Geology and Mineral Resources of the Ivanpah Quadrangle, California and Nevada.* U.S. Geological Survey Professional Paper 275. Washington, DC: U.S. Government Printing Office.

Hill, B.E., B.W. Leslie, and C.B. Connor. 1993. *A Review and Analysis of Dating Techniques for Neogene and Quaternary Volcanic Rocks*. CNWRA 93-018. San Antonio, TX: Center for Nuclear Waste Regulatory Analyses.

Ho, C.-H. 1991. Time trend analysis of basaltic volcanism at the Yucca Mountain site. *Journal of Volcanology and Geothermal Research* 46: 61–72.

Ho, C.-H. 1992. Risk assessment for the Yucca Mountain high-level nuclear waste repository site: estimation of volcanic disruption. *Mathematical Geology* 24: 347–364.

Ho, C.-H., E.I. Smith, D.L. Feurbach, and T.R. Naumann. 1991. Eruptive probability calculation for the Yucca Mountain site, USA: Statistical estimation of recurrence rates. *Bulletin of Volcanology* 54: 50–56.

Katz, M.M. 1981. *Geology and Geochemistry of the Southern Part of the Cima Volcanic Field.* M.S. Thesis. Los Angeles, CA: University of California.

Katz, M.M., and A. Boettcher. 1980. The Cima volcanic field. *Geology and Mineral Wealth of the California Desert.* D.C. Fife and A.R. Brown, eds. Santa Ana, CA: South Coast Geological Society 236–241.

Lin, C.S., R.G. Baca, and R. Drake. 1993. *VOLCANO Code — A Module for Simulation of Magmatic Scenario Model Description and User Guide*. CNWRA 93-010. San Antonio, TX: Center for Nuclear Waste Regulatory Analyses.

Margulies, T., L. Lancaster, N. Eisenberg, and L. Abramson. 1992. Probabilistic analysis of magma scenarios for assessing geologic waste repository performance. *Winter Annual Meeting.* Anaheim, CA: American Society of Mechanical Engineers.

Marsh, B.D. 1984. Mechanics and energetics of magma formation and ascension. *Explosive Volcanism: Inception, Evolution, and Hazards.* Studies in Geophysics. National Research Council/Geophysics Study Committee, eds. Washington, DC: National Academy Press: 67–83.

McBirney, A.R. 1992. Volcanology. In: *Techniques for Determining Probabilities of Geologic Events and Processes. Studies in Mathematical Geology No. 4*, R.L. Hunter and C.J. Mann, eds. International Association for Mathematical Geology. New York, NY: Oxford University Press 167–184.

McDuffie, S., C.B. Connor, and K.D. Mahrer. 1994. A simple 2D stress model of dike-fracture interaction. *Eos, Transactions of the American Geophysical Union* 75(16): 345.

Nuclear Regulatory Commission. 1991. *Disposal of High-Level Radioactive Wastes in Geologic Repositories*. Title 10, Energy, Part 60 (10 CFR Part 60). Washington, DC: U.S. Government Printing Office.

Parsons, T., and G.A. Thompson. 1992. The role of magma overpressure in suppressing earthquakes and topography: worldwide examples. *Science* 253: 1,399–1,402.

Ripley, B.D. 1981. Spatial Statistics. *Wiley Series in Probability and Mathematics*. New York, NY: John Wiley and Sons: 252.

Sheridan, M.F. 1992. A Monte Carlo technique to estimate the probability of volcanic dikes. High level radioactive waste management. *Proceedings of the Third International Conference, Las Vegas, Nevada, April 12-16, 1992.* La Grange, IL: American Nuclear Society 2: 2,033–2,038.

Sinnock, S., and R.G. Easterling. 1983. *Empirically Determined Uncertainty in Potassium-Argon Ages for Plio-Pleistocene Basalts from Crater Flat, Nye County, Nevada*. Sandia National Laboratory Report SAND 82-2441. Albuquerque, NM: Sandia National Laboratory.

Smith, R.L., and R.G. Luedke. 1984. Potentially active volcanic lineaments and loci in western conterminous United States. *Explosive Volcanism: Inception, Evolution, and Hazards*. National Research Council/Geophysics Study Committee, eds. Studies in Geophysics. Washington, DC: National Academy Press 47–66.

Smith, E.I., T.R. Feuerbach, and J.E. Faulds. 1990. The area of most recent volcanism near Yucca Mountain, Nevada: Implications for volcanic risk assessment. High-level radioactive waste meeting. *Proceedings of the International Topical Meeting*. La Grange Park, IL: American Nuclear Society 1: 81–90.

Stirewalt, G.L., S.R. Young, and K.D. Mahrer. 1992. *A Review of Pertinent Literature on Volcanic-Magmatic and Tectonic History of the Basin and Range*. CNWRA 92-025. San Antonio, TX: Center for Nuclear Waste Regulatory Analyses.

Turrin, B.D., J.C. Dohrenwend, R.E. Drake, and G.H. Curtis. 1985. K-Ar ages from the Cima volcanic field, eastern Mojave Desert, California. *Isochron/West* 44: 9–16.

Turrin, B.D., D. Champion, and R.J. Fleck. 1991. $^{40}Ar/^{39}Ar$ age of the Lathrop Wells volcanic center, Yucca Mountain, Nevada. *Science* 253: 654–657.

Ulrich, G.E., C.D. Condit, K.J. Wenrich, E.W. Wolfe, R.F. Holm, L.D.Nealey, F.M. Conway, J.C. Aubele, and L.S. Crumpler. 1989. Miocene to Holocene volcanism and tectonism of the southern Colorado Plateau, Arizona. *New Mexico Bureau of Mines and Mineral Resources Memoir* 46: 1–41.

U.S. Environmental Protection Agency. 1991. *Environmental Radiation Protection Standards for Management and Disposal of Spent Nuclear Fuel, High-Level and Transuranic Radioactive Wastes.* Title 40, Protection of Environment, Part 191 (40 CFR Part 191). Washington, DC: U.S. Government Printing Office.

Wallman, P.C. 1994. *Sensitivity Studies on Volcanic Hazard at Yucca Mountain.* Presentation to the Nuclear Waste Technical Review Board, Panel on Structural Geology and Geoengineering. Meeting on Probabilistic Seismic and Volcanic Hazard Estimation. San Francisco, CA.

Wang, C.H., D.L. Willis, and W.D. Loveland. 1975. *Radiotracer Methodology in the Biological, Environmental, and Physical Sciences.* Englewood Cliffs, NJ: Prentice-Hall, Inc.

Wells, S.G., J.C. Dohrenwend, L.D. McFadden, B.D. Turrin, and K.D. Mahrer. 1985. Late Cenozoic landscape evolution on lava flow surfaces of the Cima volcanic field, Mojave Desert, California. *Geological Society of America Bulletin* 96: 1,518–1,529.

Wilshire, H.G. 1986. Xenoliths of the Cima volcanic field, California. *Geological Society of America Abstracts with Programs* 18(2): 199.